AD-A151 704 WIDEBAND FIBER OPTIC COMMUNICATIONS LINK(U) AIR FORCE 1/2
INST OF TECH WRIGHT-PATTERSON AFB OH SCHOOL OF
ENGINEERING J R BRAY DEC 84 AFIT/GE/ENG/84D-16

UNCLASSIFIED F/G 17/2 NL

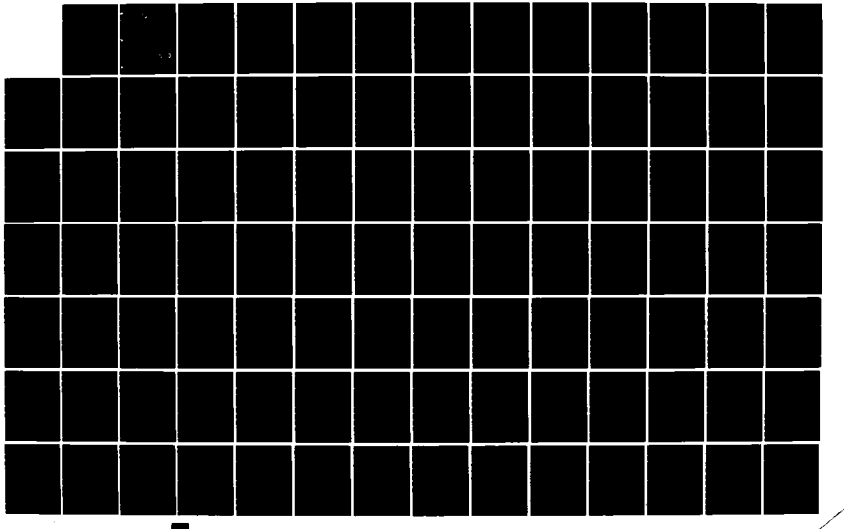

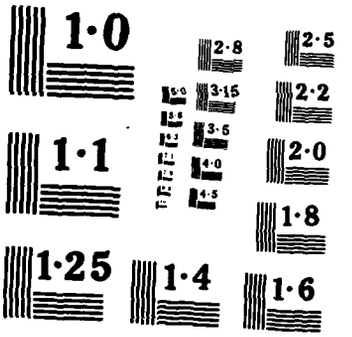
1·0
2·8
2·5
3·15
2·2
3·5
1·1
4·0
2·0
4·5
1·8
1·25
1·4
1·6

AD-A151 704

WIDEBAND FIBER OPTIC COMMUNICATIONS LINK

THESIS

James R. Bray
First Lieutenant, USAF

AFIT/GE/ENG/84D-16

DTIC FILE COPY

DISTRIBUTION STATEMENT A
Approved for public release;
Distribution Unlimited

DTIC
ELECTE
MAR 2 8 1985
S D
B

DEPARTMENT OF THE AIR FORCE
AIR UNIVERSITY
AIR FORCE INSTITUTE OF TECHNOLOGY

Wright-Patterson Air Force Base, Ohio

85 03 13 135

REPRODUCED AT GOVERNMENT EXPENSE

AFIT/GE/ENG/84D-16

WIDEBAND FIBER OPTIC

COMMUNICATIONS LINK

THESIS

James R. Bray
First Lieutenant, USAF

AFIT/GE/ENG/84D-16

DTIC
ELECTE
MAR 2 8 1985
S
B

DISTRIBUTION STATEMENT A
Approved for public release
Distribution Unlimited

AFIT/GE/ENG/84D-16

WIDEBAND FIBER OPTIC COMMUNICATIONS LINK

THESIS

Presented to the Faculty of the School of Engineering

of the Air Force Institute of Technology

Air University

In Partial Fulfillment of the

Requirements for the Degree of

Master of Science in Electrical Engineering

James R. Bray, B.S.

First Lieutenant, USAF

December 1984

Approved for public release; distribution unlimited

Preface

The purpose of this study was to design and implement a single strand, full duplex, fiber optic communications link. The finished system, complete with user's manual and schematics, is to remain at the Air Force Institute of Technology for future research and experimentation.

This fiber optic project demonstrates the ease and practicality of using fibers for ground based local or long haul communications systems. However the first four references listed in the bibliography show other uses, primarily on aircraft systems, accenting potential use in a military environment.

Because of over eight years experience in both long line and radio propagation communication systems I completed the work on this project with great interest and enthusiasm. I also believe that this type of project compliments and completes the Optical Communications Course Sequence that I completed at AFIT.

I would like to thank Major Kenneth C. Castor for suggesting and allowing me to do this work, and Dr. Vaqar Syed for the freedom to pursue my self imposed goals throughout the project. Finally, I wish to thank my wife Conchi and my daughters, Elena and Sole, for their support and understanding through these nine long months of this project.

James R. Bray

Table of Contents

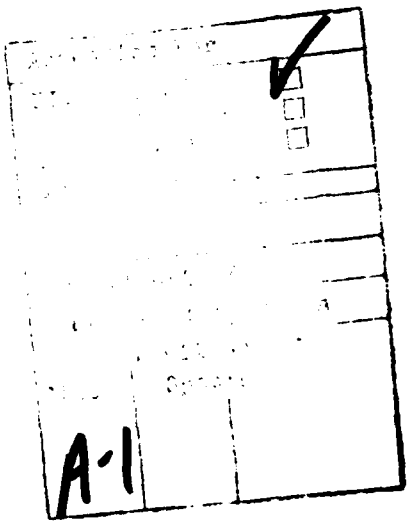

List of Figures

List of Tables

Abstract

A feasibility study was conducted on the possibility of upgrading a nine port fiber optic bundle telecommunications system to a single strand fiber optic system. Usable pieces of equipment were identified and new Light Emitting Diodes (LED), Photodetectors and single strand SMA styled fiber optic connectors were ordered. Background research was conducted in the area of fiber optic power launching, fiber losses, connector losses and efficiences. A new modulation/demodulation circuit was designed and constructed using parts from unused equipment. A new front panel was constructed to house the components, switches and connectors. A two meter piece of optical fiber was terminated with the new connectors and tested for connector loss, numeric aperture and attenuation. The new Light Emitting Diode was characterized by its emission radiation pattern and the entire system was tested for functional operation, frequency response and bandwidth of operation. An Operations Manual was prepared to ensure proper use in the future. The result was a two piece, single strand, fiber optic communications system fully TTL compatible, capable of transmitting digital signals from 80 Kbit/sec to 20 Mbit/sec. The system was tested in a half duplex mode using both baseband and carrier modulated signals. Utilizing both pieces of the system full duplex operation was also demonstrated.

WIDEBAND FIBER OPTIC COMMUNICATIONS LINK

I. Introduction

In October, 1973, Spectronics, Inc. was contracted to develop a program concerned with the design and fabrication of an Electro-Magnetic Interference/Electro-Magnetic Pulse Resistant Data Bus. The system was constructed as an opto-electronic data bus and was compared to systems using twisted pair, coaxial cable and waveguide communications media. The system constructed used GaAs Light Emitting Diodes, flexible Fiber Optic Bundles, Silicon PIN Photodiodes and passive optical couplers. This fiber optic system was delivered to the Air Force Avionics Laboratory at Wright-Patterson Air Force Base in September, 1975. When the Avionics Lab finished their work with the system, all remaining equipment, documents and schematics were given to the Air Force Institute of Technology for research and experimentation.

An investigation was conducted on the remaining equipment from the Spectronics Data Bus to determine the feasibility of upgrading the system to a single strand optical fiber communications link. The investigation entailed determining whether the system was operational or not, its protocol system and the practicality of its coding scheme. The system's electro-optic interface was also checked for its compatibility with a single strand optical fiber. Research was con-

ducted on optical fibers themselves in the areas of power launching techniques and efficiency, coupling loss, intrinsic losses and bandwidth constraints.

It was determined that a single strand optical fiber communications system could be implemented utilizing much of the equipment provided by the Spectronics project with only a few major changes. The original protocol and coding schemes were not versatile enough and were to be eliminated along with the existing electro-optic interface and fiber optic bundles. New single strand fibers with standard connectors were to be constructed and new Light Emitting Diodes and Photodetectors were ordered to be installed on the cabinet. A modulation/demodulation circuit was to be designed and constructed to provide a system capability of both baseband and carrier modulation modes of transmission. The system was designed to operate on digital signals at least as fast as the original system, 10 Mbit/sec, Manchester NRZ code.

Once implemented the system was to be tested at both the component level and for overall system operation. Finally, a user's manual was to be prepared to ensure proper use of the new system in subsequent research and experimentation.

II. Background Information

Research for this project was conducted and is presented in four major categories. First, a discussion on the feasibility of upgrading some in-house available equipment from fiber bundle to single strand fiber optic communications media. Next, is a presentation of fiber optic power losses and bandwidth considerations. This is followed by a discussion of Light Emitting Diodes, Laser Diodes and Photodetectors, and finally, a series of tests that can be used to characterize a completed fiber optic communications link and its primary components.

Description of Available Equipment

In September, 1976, Technical Report AFAL-TR-76-99 was submitted to the Air Force Avionics Laboratory along with all equipment that comprised an Electro-Magnetic Interference/ Electro-Magnetic Pulse (EMI/EMP) Resistant Data Bus. This system was designed using fiber optic bundle technology and was completed by Spectronics, Inc., of Richardson, Texas.

When the Air Force Avionics Laboratory completed their work with the EMI/EMP Resistant Data Bus the remaining equipment was given to the Air Force Institute of Technology (AFIT). Table I lists the equipment originally supplied by Spectronics and also shows the quantities that remain on hand at AFIT now. All remaining equipment and the final report are now located and available, with schematics, in the

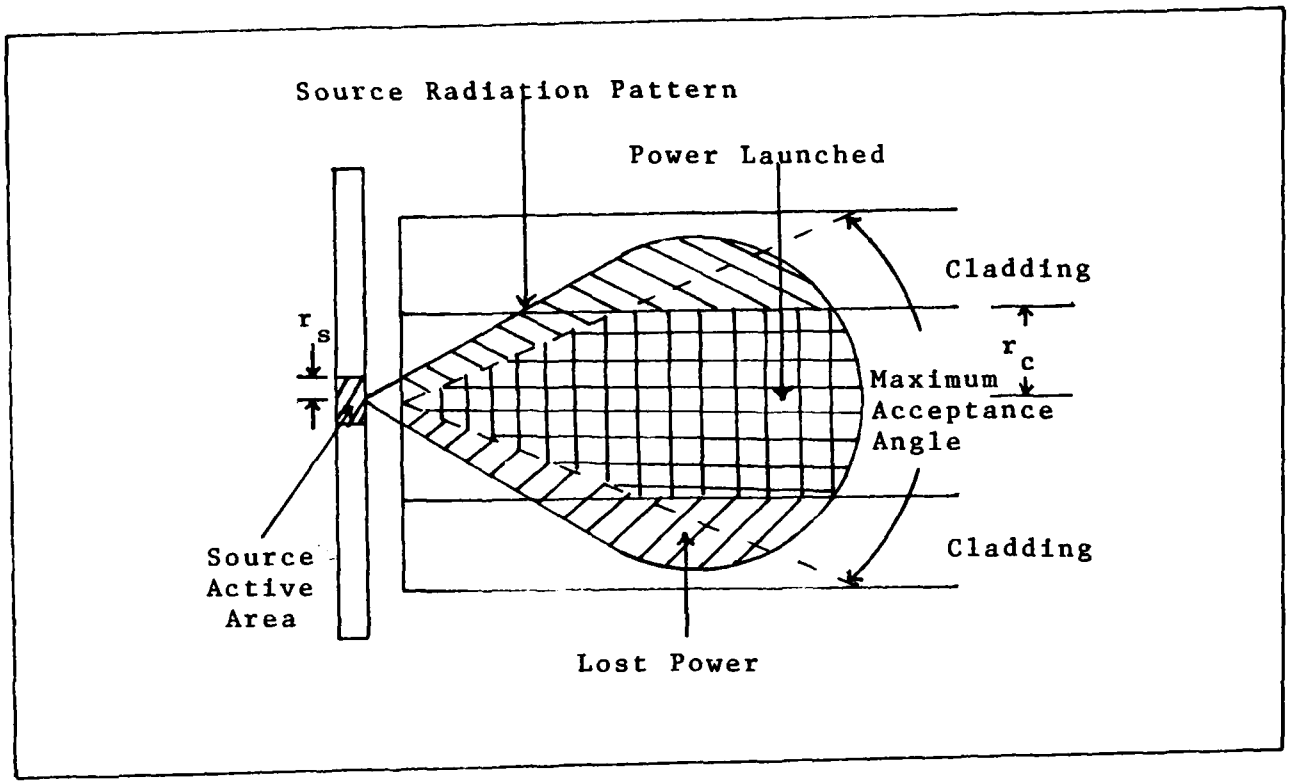

(11:121)

Figure 5. Optical Power Launching.

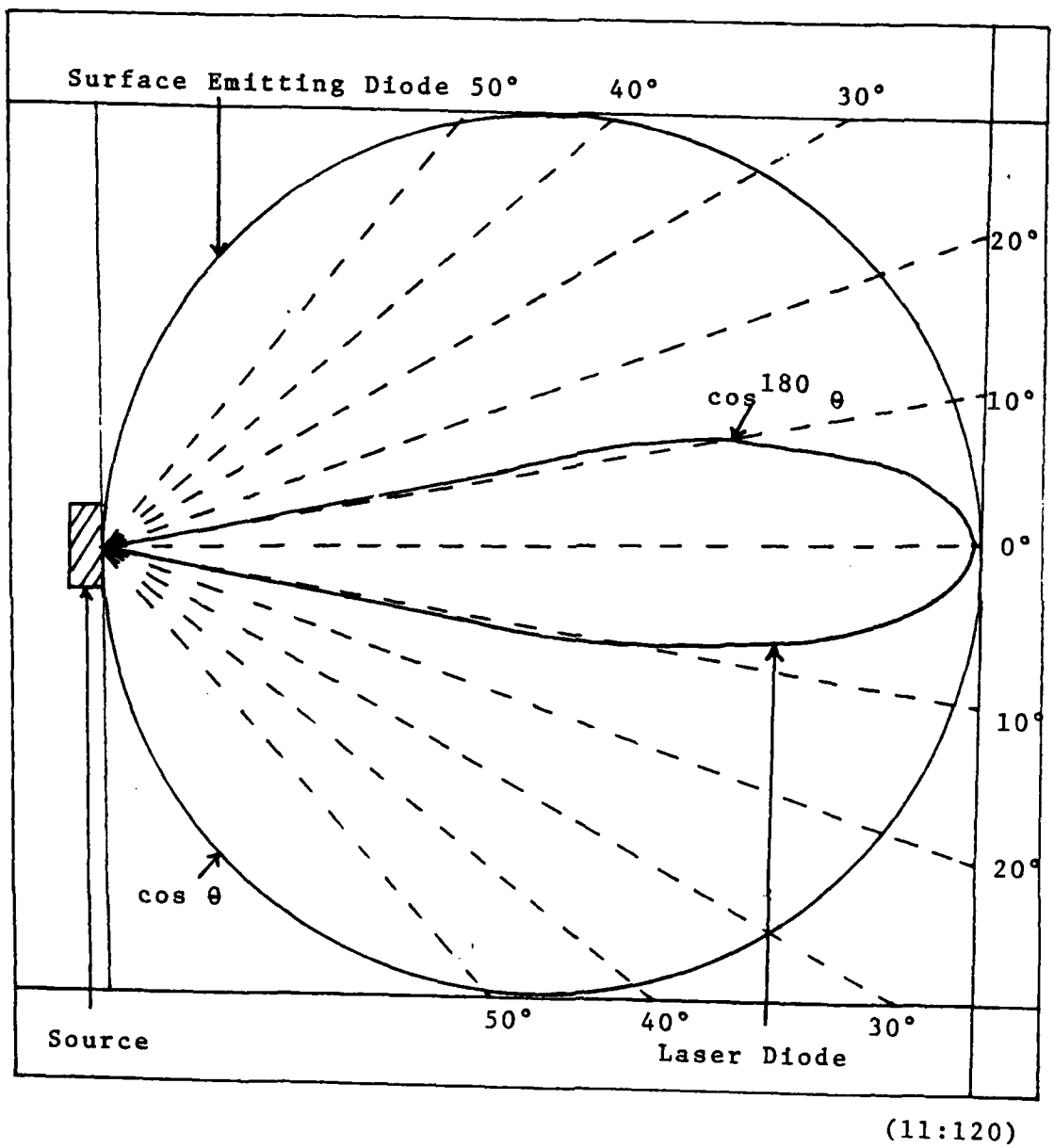

Figure 4. Radiance Power Beams of Surface Emitting and Laser Diode.

are normally modeled as pure Lambertian sources; however, edge emitting LED's and laser diodes are somewhat more complicated to model. Equations (1) and (2) below are the mathematical descriptions of the output radiance patterns of the surface emitting and edge emitting LED's (11:120).

$$B(\theta,\phi) = B_o \cos\theta. \tag{1}$$

$$\frac{1}{B(\theta,\phi)} = \frac{\sin^2\phi}{B_o \cos^T(\theta)} + \frac{\cos^2\phi}{B_o \cos^L(\theta)}. \tag{2}$$

The term B_o is the maximum radiance emitted by the source. The angles θ and ϕ are the same as those normally defined in spherical coordinates. The terms T and L are the transverse and lateral power distribution coefficients. For edge emitting diodes, the (parameter) T of Equation (2) is normally 1, while the (parameter) L is significantly larger. Figure 4 is an example of both the surface emitting diode and a laser diode output radiation patterns. The laser diode has a half-power beam width of 10°, where L is approximately 180. The magnitude of the laser diode has been greatly reduced in order to put both diagrams on the same chart.

An example of a theoretical calculation of the amount of power that can be launched into a fiber will be shown with a step index fiber as depicted in Figure 5. The amount of power actually coupled to the fiber, P_f, can be determined from Equation (3).

desirable because the 37 strand Valtec fiber bundle was split with 19 strands for the transmit side and 18 strands for the receive.

The optical fiber bundles for the EMI/EMP Data Bus were interconnected with a nine port radial coupler. This optical connector had the property of splitting the input signal from any of the ports to all nine fiber bundles of the system. The optical coupler is still intact, complete with test data and connecting plug.

Also available at AFIT are three spools of single strand optical fiber. One spool is identified with the part number ITT-T-1271-16. This fiber has a 50μm core, 125μm outer diameter, Numeric Aperture (NA) of 0.2, parabolically graded index of refraction, approximately 3 dB/Km loss and is about 200 meters in length. The other two spools have considerably less fiber and are not marked with any identifying part numbers.

Optical Fibers

Discussion on optical fibers will be limited to single strand, multi-mode fibers, their power launching capabilities, power losses and bandwidth limitations. Then comparisons of fibers on hand and some commercially available fibers will be presented.

The amount of optical power that can be successfully launched into a fiber is dependent not only on the fiber itself, but also on the power source. Surface emitting LED's

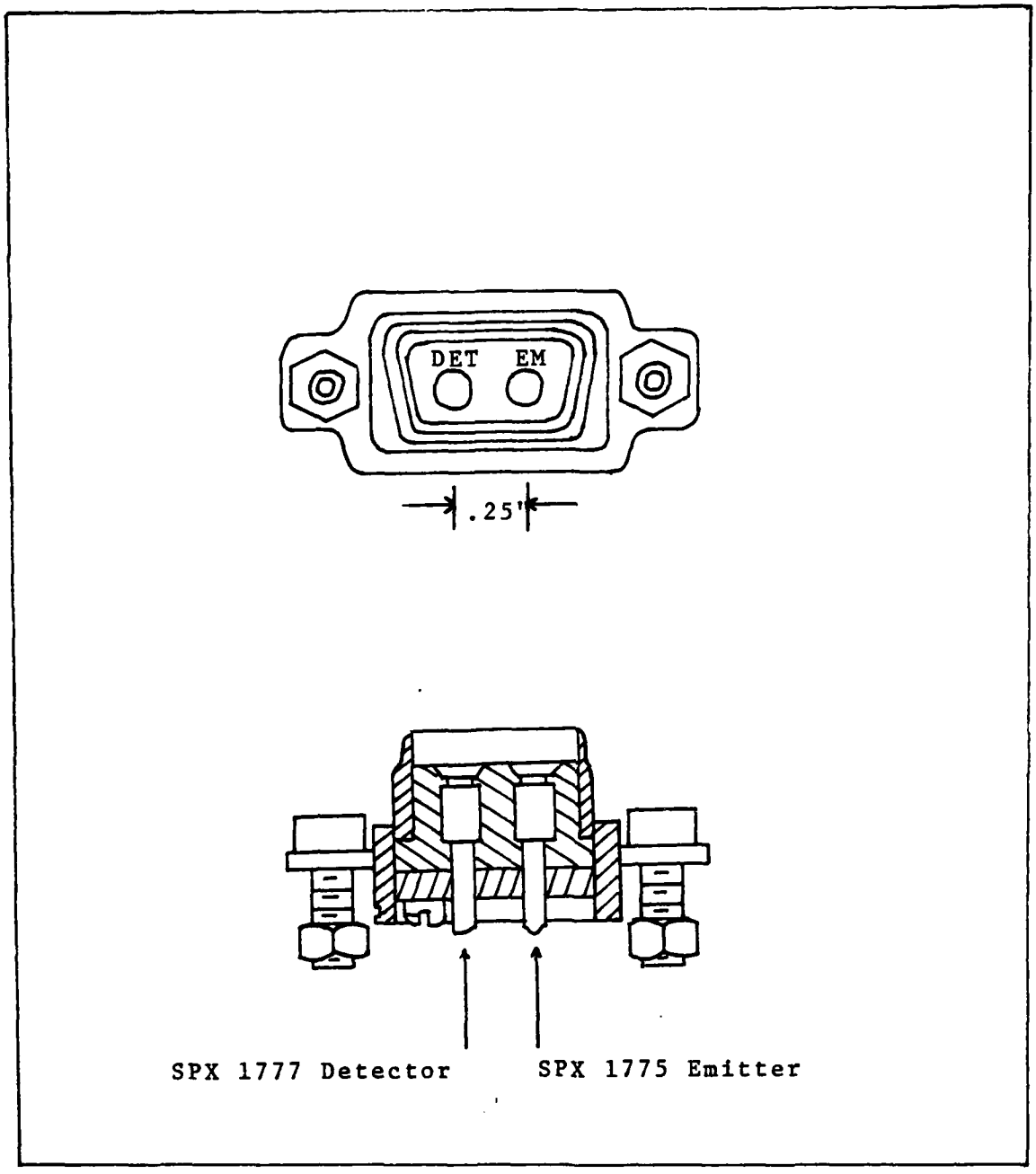

(1:36)

Figure 3. ITT Connector.

munications experiments.

Another severe limitation for the use of this system as originally designed is that the MTU Test Sets were not delivered to AFIT as part of the package. At least one of these test sets is essential because it generates a status word back to the CMTU after the initial command word. Without this status word, data transmission is prohibited by the CMTU.

Lastly, the CMTU and the CMTU Test Set were checked for circuit integrity and were found to be modified from their original design. Specifically, the serial data stream line from the parallel to serial convertor card to the LED driver/amplifier card in the CMTU had been cut allowing a direct TTL compatible input to the optical transmitter. Also, the data stream line from the PD detector card to the signal conditioning card had been cut allowing a direct TTL compatible data line from the optical receiver. Further inspection of the interface between the CMTU Test Set and the CMTU showed that the command logic between these two components was not functioning properly. When the CMTU would query the CMTU Test Set for a specific response to set up a data transfer, there was no response.

The LED's and PD's were mounted to the CMTU and MTU's with a modified connector manufactured by ITT Cannon Electric Division. This connector is shown in Figure 3. The advantage of this connector for this specific purpose was the close proximity of the LED and PD terminations. This was

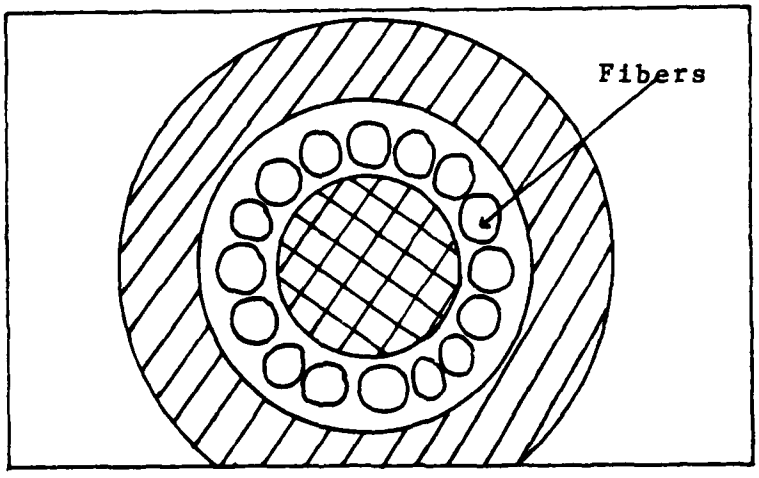

Figure 2a. Ring Termination for LED Interface.

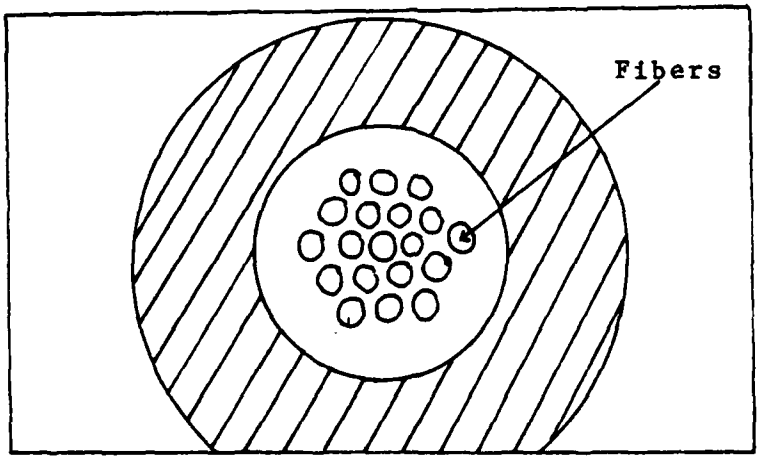

Figure 2b. Circular Termination for Photodiode Interface.

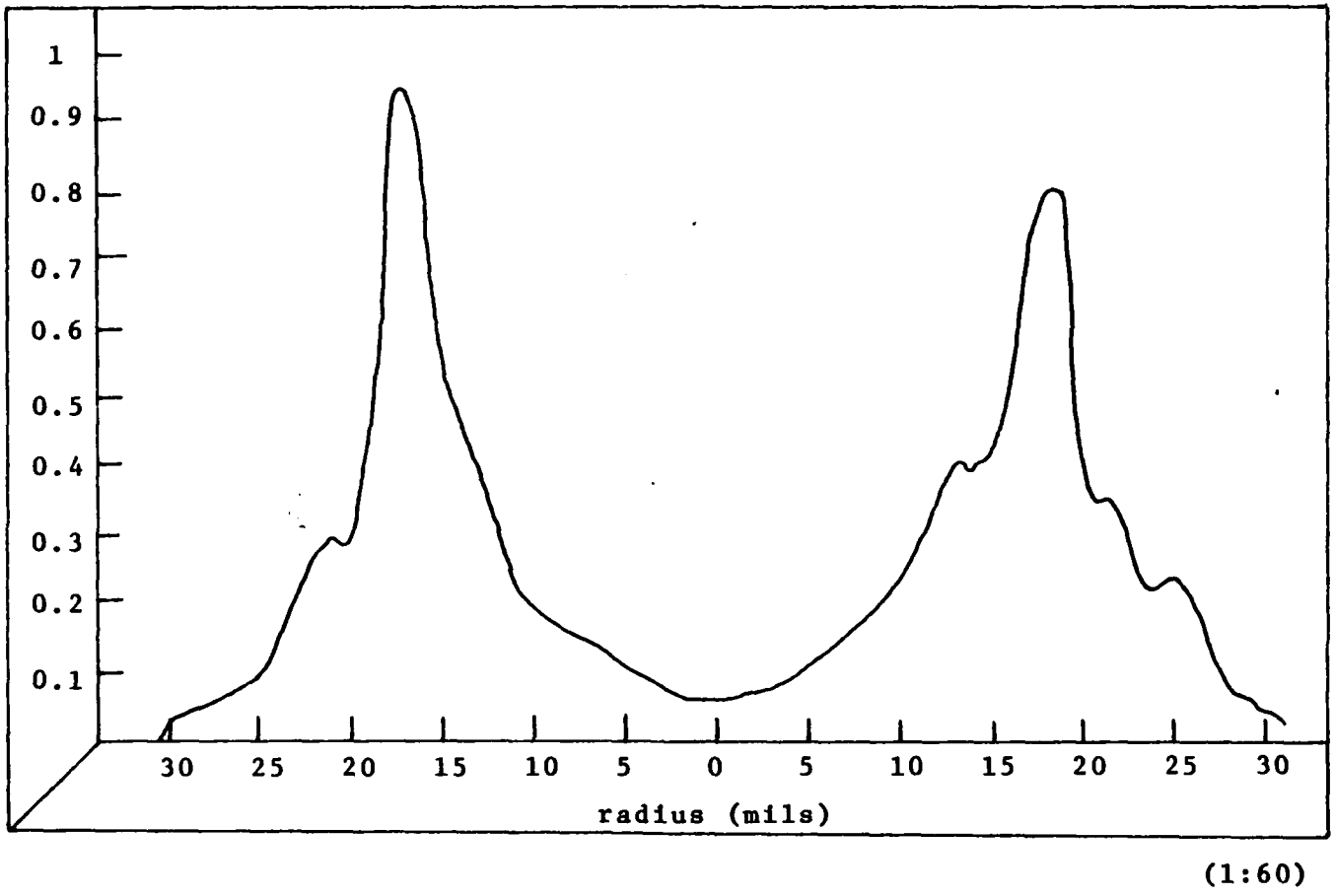

Figure 1. SPX 1775 Output Intensity vs Radius.

Table IV

Specifications for Valtec Fiber Bundles

Number of fibers	37
Fiber diameter	5.0 mils ± 10%
Core diameter	4.0 mils ± 10%
Jacket	63 Durometer Hytrel 0.11 OD
Numeric Aperture	0.3
Attenuation	100dB/Km @ 907nm

(1:55)

Table III

SPX 1777

Description:	p-i-n Photodiode Coaxial package
Chip thickness	0.004 in (nominal)
Active area	0.050 in diameter

Optical/Electrical Specifications @ 25°C.

	Min	Max	Typical
Reverse breakdown voltage @ I_R = 10μa	180V	200V	
Dark leakage current @ V_R = 90V		20nA	1nA
Total Capacitance @ V_R = 90V		4.2pF	
1MHz @ V_R = 30V		5.2pF	
Responsivity @ 907nm	0.5A/W		
Rise Time (10 - 90%) @ V_R = 90V		1.5ns	
Series resistance (cal) @ V_R = 90V		15Ω	

(1:34)

Table II

SPX 1775

Description:	GaAs Edge Emitting LED		
Optical/Electrical Specifications @ 25°C.			
	Min	Max	Typical
Reverse breakdown voltage @ I_R = 10μa	4.0V		
Forward voltage @ I_F = 100ma		1.5V	
r_s			1.0Ω
C_T @ V_R + 1V, f = 1MHz			12pf
τ_ρ @ 100ma			907nm
$\Delta\tau$ @ 100ma			22nm
Power out	2.0mW		
θ = 15° half angle $f_o p_\theta$			1mW
tr			20ns

(1:34)

Tables II,III and IV.

The Spectronics SPX 1775 LED has an output intensity vs radius radiation pattern that lends itself very well to use with optical fiber bundles. As shown in Figure 1, the output intensity is greatest approximately 17.5 mils distant from the center axis of the LED. To achieve maximum power transfer into the Valtec fiber bundle the fiber cable was terminated as shown in Figure 2a. For termination into the PD, the fibers were collected as close to the axial center as possible, thus putting the maximum amount of optical power on the active area of the detector. This configuration is shown in Figure 2b.

The Spectronics system seemed ideal for use as an experimental fiber optic transmission media with some specific inherent limitations. First, the system was designed for use with fiber optic bundles rather than single strand optical fiber cable. Recent technology has gone to single fiber because of improvements in fiber loss characteristics which enables longer transmission lengths with less physical size and weight, and wider bandwidths at a cost lower than that of the multi-strand fiber bundles. The Spectronics system of time division multiplexing made other types of modulation and multiplexing impractical because of the strict protocol involved with the command and status words. Even if the command and status word logic could be by-passed, the sync pulse and parity check assignments in the data words made this mode of transmission unattractive for more advanced com-

Communications-Electronics Laboratory at AFIT.

This fiber optic data bus was designed as a 10Mbit, eight user, time division multiplex system with all data transfers controlled by the CMTU. The MTU's served as the electronic/fiber optic interface units for the subsystems or users.

The system was capable of transferring data from the controller to the user, user to controller, and from user to user. Data transfer was accomplished through the use of three types of words. First, a command word that identified the terminals involved, transmit/receive, number of data words to be transmitted, parity check and a synchronous timing pulse. Second, the status word that contained a sync pulse, parity check, Subsystem Interface Unit (SSIU) status bit, parity error bit, terminal identifying address bits and nine MTU failure code bits. And finally, the data word that contained a sync pulse, parity check bit and 16 data bits.

The CMTU Test Set was designed as a Bit Error Rate (BER) Test Set by transmitting the parity error bit from the status word to a detector circuit, then to an external connection which could be coupled to a standard counter. The number of bits transmitted was controlled by the length of time the test was in progress and by knowing the transmission rate.

The optical transmission media was comprised of Spectronics SPX 1775 Light Emitting Diodes (LED), Spectronics SPX 1777 p-i-n Photodetectors (PD) and Valtec Fiber Bundles. Pertinent data for these three components are listed in

Table I

EMI/EMP Resistant Data Bus Equipment

Quantity Originally Supplied	Nomenclature	Quantity Remaining
7	Multiplex Terminal Unit (MTU)	3
1	Control Multiplex Terminal Unit (CMTU)	1
2	MTU Test Set	0
1	CMTU Test Set	1
1	9 Port Radial Coupler	1
1	Fiber Optics Radial Coupler Cable Assembly Consisting of 2 each: 10 ft. fiber optic cable 20 ft. fiber optic cable 30 ft. fiber optic cable 50 ft. fiber optic cable	1
2	Subsystem Interface Unit/MTU Interface Cable	0
1	Controller/CMTU Interface Cable	0
6	Transit cases	0
3	Power outlet strips	0

(1:5)

$$P_f = \int_0^{r_m} \int_0^{2\pi} [\int_0^{2\pi} \int_0^{\theta_{max}} B(\theta,\phi)\sin\theta d\theta d\phi] r d\theta_s dr. \quad (3)$$

In Equation (3), the radiance from an individual point is integrated over the acceptance angle θ of the fiber (the term inside the square brackets). The total power is then obtained by summing over all points on the active area of the diode. In the case of a pure Lambertian source, $B(\theta,\phi)$ is replaced with $B_o\cos\theta$, and Equation (3) then reduces to

$$P_{f,step} = \pi^2 r_s^2 B_o (NA)^2, \quad (4)$$

when the radius of the source, r_s, is smaller than the radius of the fiber core, r_c. When the radius of the fiber core is smaller than the radius of the source, Equation (3) becomes

$$P_{f,step} = \pi^2 (\frac{r_c}{r_s})^2 B_o (NA)^2. \quad (5)$$

In Equations (4) and (5) the term "NA" is the Numeric Aperture of the fiber and is defined by

$$NA = \sin\theta_{max} = (n_1^2 - n_2^2)^{1/2}, \quad (6)$$

where n_1 and n_2 are the refractive indices of the fiber core and cladding respectively.

For graded index fibers the amount of power coupled to the fiber is determined to be (11:122)

$$P_{f,graded} = 2\pi^2 r_s^2 B_o n_1^2 \Delta [1 - \frac{2}{a+2}(\frac{r_s}{r_c})^a]. \quad (7)$$

The term Δ is defined by

$$\Delta = \frac{n_1 - n_2}{n_1}, \qquad (8)$$

and "a" is the index profile coefficient.

It can be seen from this discussion that the amount of power coupled to a fiber is primarily a function of the geometry of the source and the fiber, and the fiber's numeric aperture. Additional losses can occur at the launching point if the fiber face is misaligned, has high reflectance or if there is an axial misalignment between the source and fiber.

In the following discussion on fiber to fiber coupling losses several assumptions are made. Foremost of these assumptions is that the reader has a good understanding of electromagnetic mode propagation in a waveguide. The other assumptions are that all modes propagating in the fiber are equally excited and the geometries of the fibers and source are ideal. That is, if the cross section of the fiber is depicted as circular, then it is treated as a perfect circle, the step change in index of refraction between the fiber core and cladding is treated as a perfect step and that the core/cladding interface could be depicted as a smooth surface longitudinally down the fiber.

As an example of fiber to fiber coupling loss, consider two multi-mode, step index fiber with equal core diameters joined in a dry connector. The major causes of power loss in this example are three mechanical misalignments: axial displacement, longitudinal separation, and angular misalign-

ment.

Axial displacement is the most important of the three misalignments and will be discussed first. If all modes propagating in the fiber are equally excited, then the percentage of power coupled to the receiving fiber is equal to the common area of the two fiber cores. Figure 6 depicts this overlapping effect when the axial displacement is equal to an amount "d". The area of the fiber core is πr_c^2 and the common core area is given by Equation (9).

$$A_{comm} = 2r_c^2 \cos^{-1}\left(\frac{d}{2r_c}\right) - d\left(r_c^2 - \frac{d^2}{4}\right)^{1/2}. \qquad (9)$$

An inspection of Equation (9) shows that as the displacement approaches twice the magnitude of the core radius the common area, and therefore the power coupled, goes to zero.

Axial displacement loss for graded index, or step to graded index fibers is considerably more involved. The reason for the increased complication is that the controlling factor at the coupling point is the smaller of the two numeric apertures. The changing numeric aperture is a function of the distance from the fiber axis. Not only is the common core area integrated but the smaller of the two numeric apertures must be integrated on a point to point basis to determine the number of modes that can propagate in both fibers.

For a graded index to graded index connection of identical fibers, with a grading index profile coefficient a equal to 2, and with the axial displacement much smaller than

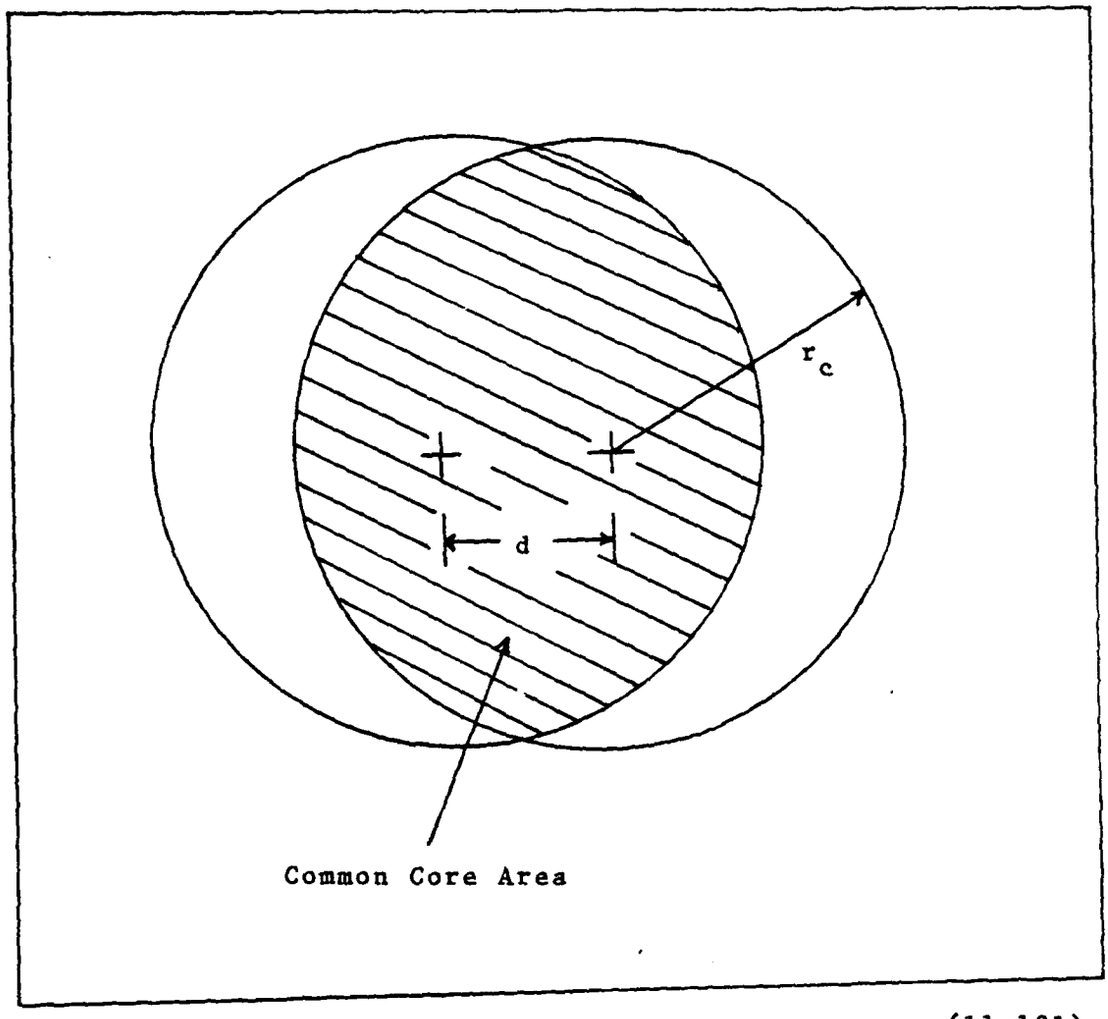

(11:131)

Figure 6. Axial Displacement

the radius of the core, the power to the receiving fiber can be approximated by (11:134)

$$P_{f,graded} = P_s(1 - \frac{8d}{3\pi r_c}). \quad (10)$$

The term P_s in Equation (10) is the total power exiting the emitting fiber.

Power loss due to longitudinal separation is much less complicated to calculate, and compared to axial displacement, causes less loss as the displacement "d" increases. As an example, consider the two identical step index fibers depicted in Figure 7, separated by a longitudinal separation "d". Again, with all modes equally excited, the percentage of power coupled to the receiving fiber is equal to the ratio of the core area to the area of the expanding beam. The beam expands at the same angle θ_{max}, as the maximum acceptance angle at the entrance of the fiber. This simple ratio comes from the assumption of equally excited modes because, since the fibers are identical, they both support the same number of modes, and only those modes that reach the receiving fiber's core face are coupled.

Angular misalignment is mathematically the most complicated of the three mechanical misalignments, but with a small angular displacement this also accounts for the smallest of the power losses.

The theoretical loss for two identical step index fibers with an angular misalignment has been calculated to be (11:134)

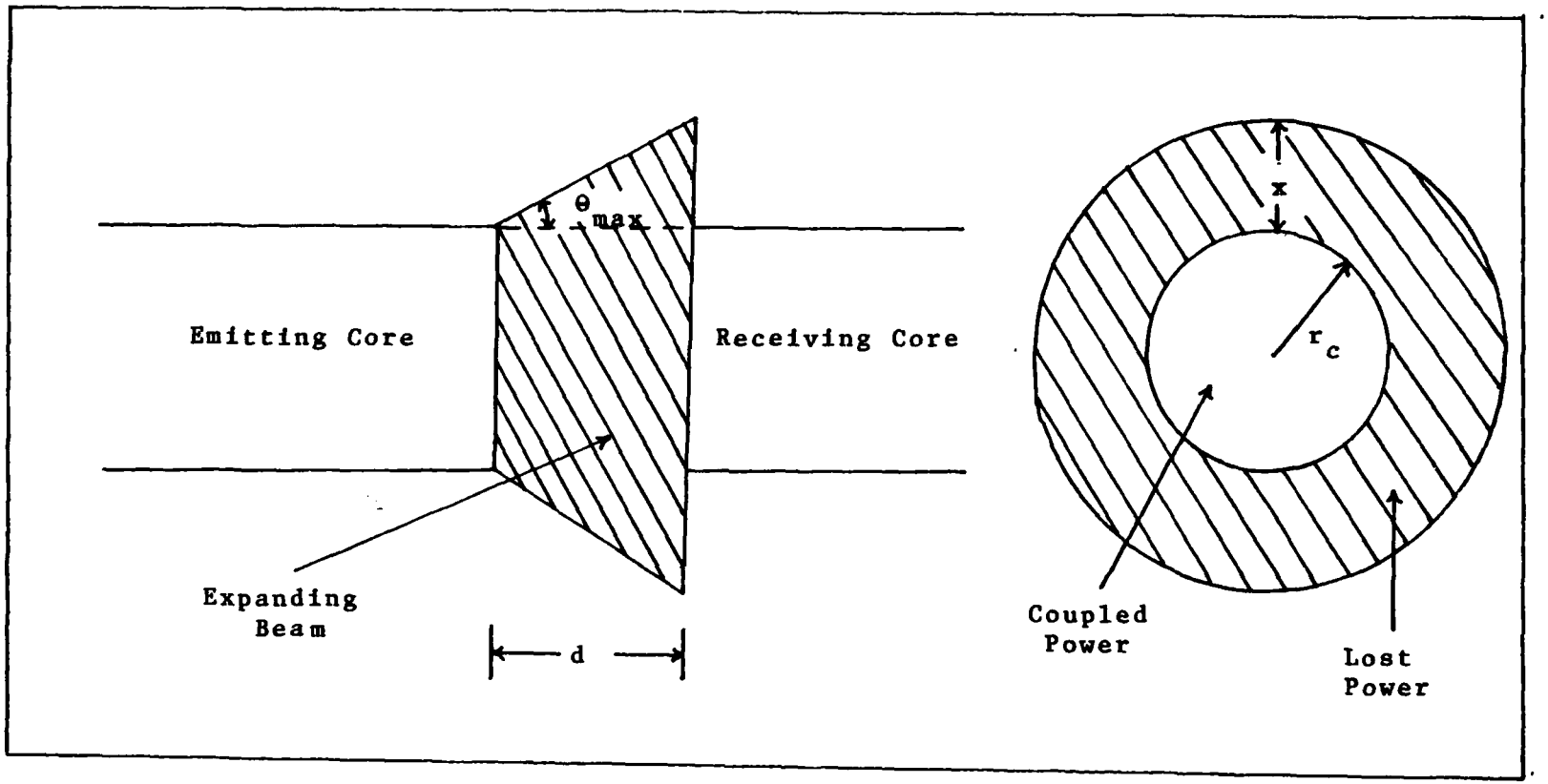

(11:134)

Figure 7. Longitudinal Separation.

$$\text{Loss} = -10\log(\cos\theta[\tfrac{1}{2} - \tfrac{1}{\pi}p(1 - p^2)^{1/2} - \tfrac{1}{\pi}\sin^{-1}(p) - q(\tfrac{1}{\pi}y[1 - y^2]^{1/2} + \tfrac{1}{\pi}\sin^{-1}(y) + \tfrac{1}{2})]). \quad (11)$$

This loss is in decibels and p,q and y are defined as

$$p = \frac{\cos\theta_{max}(1 - \cos\theta)}{\sin\theta_{max}\sin\theta} \quad (12)$$

$$q = \frac{\cos^3\theta_{max}}{(\cos^2\theta_{max} - \sin^2\theta)^{3/2}} \quad (13)$$

$$y = \frac{\cos^2\theta_{max}(1 - \cos\theta) - \sin^2\theta}{\sin\theta_{max}\cos\theta_{max}\sin\theta} \quad (14)$$

Each of these three mechanical misalignments were calculated as though the other two did not exist. However, they normally all exist simultaneously but can be treated independently.

Three other minor causes of power loss are differences in core radii, numeric apertures and graded index profiles. These losses are given by the following three equations in which the subscripts "e" and "r" refer to emitting and receiving fibers (11:136).

$$L(r) = \begin{cases} -10\log(\frac{r_r}{r_e})^2 & \text{for } r_r \text{ less than } r_e \\ 0 & \text{for } r_e \text{ less than } r_r \end{cases} \quad (15)$$

$$L(NA) = \begin{cases} -10\log(\frac{NA_r(0)}{NA_e(0)})^2 & \text{for } NA_r \text{ less than } NA_e \\ 0 & \text{for } NA_e \text{ less than } NA_r \end{cases} \quad (16)$$

$$L(a) = \begin{cases} -10\log\left(\frac{a_r(a_e+2)}{a_e(a_r+2)}\right) & \text{for } a_r \text{ less than } a_e \\ 0 & \text{for } a_e \text{ less than } a_r \end{cases} \quad (17)$$

Power loss is not restricted to fiber connections and source to fiber power launching techniques. The fibers themselves have intrinsic losses that can be categorized into three classes: absorbtion, scattering and radiative losses. These three types of losses are generally lumped together and defined as the attenuation coefficient of the fiber and is measured in decibels per kilometer.

Absorbtion losses are caused by impurities in the glass of the fiber. Impurities such as iron, cobalt, chromium, copper and water ions (OH) cause absorbtion by the fiber in the wavelength region of the optical source. The Vapor Phase Deposition method of fabricating optical fibers creates glass with impurity counts that are only one percent of those made by the Direct Melt method (9). Doping the glass with materials such as germanium-oxide are often used to reduce the effects of the impurities(16).

Scattering losses arise from microscopic variations in material density. Also, since fibers contain oxides like Silicon-oxide and Germanium-oxide, the index of refraction varies over distances that are small compared to the wavelength of the optical power source.

Radiative losses occur whenever there is a bend in the fiber. Fiber bends occur in two forms; first, when the bend

radius is much larger that the fiber diameter, and the second which is due to the microscopic bends or variations at the core-cladding interface.

The first of these radiative losses is explained with Figure 8. In this drawing "R" represents the bend radius and only the lowest order mode propagating is depicted. The evanescent field in the cladding decays exponentially as a function of the distance from the core axis. The field tail moves along with the field in the core; therefore when the fiber is bent the tail must move faster. At a certain critical distance x_c, the tail would have to move faster than the speed of light to keep up. Since this is impossible, the field tail radiates away. Higher order modes radiate away faster because their field tails in the cladding are proportionally larger than the lower order modes. Fiber bends can be used as fiber optic attenuators or mode controlling filters because the tighter the fiber is bent the more modes and power can be radiated away.

Microbends in fibers causing radiative losses are shown in Figure 9. They can be caused from packaging faults while jacketing the fiber or from external forces on the fiber cable. The loss from these microbends is explained in the same manner as for the larger fiber bends. Microscopic variations at the core-cladding interface can change the angle of reflection within the core and therefore create a mode conversion. If the new mode that was just created cannot be supported by the fiber then it will radiate away through the

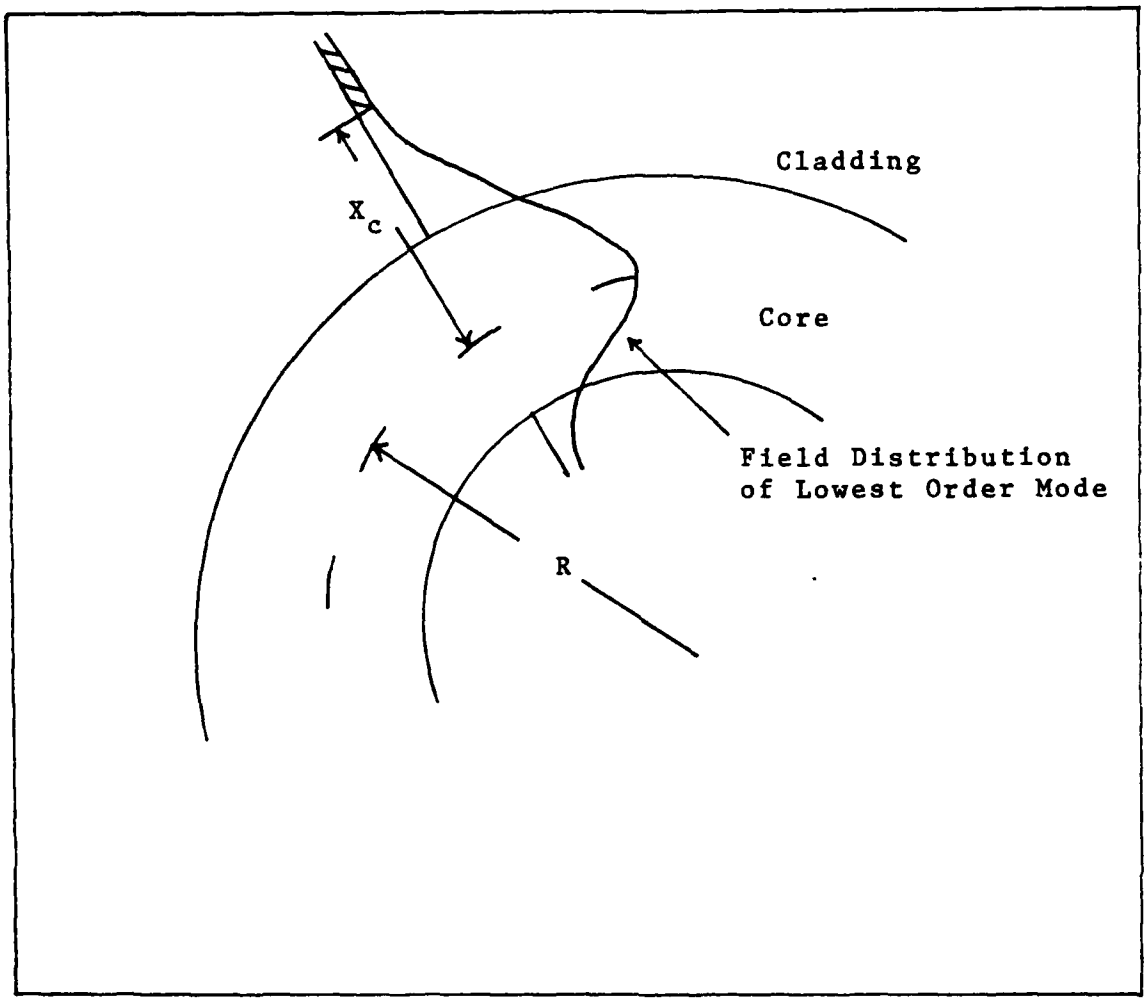

(11:56)

Figure 8. Radiative Loss.

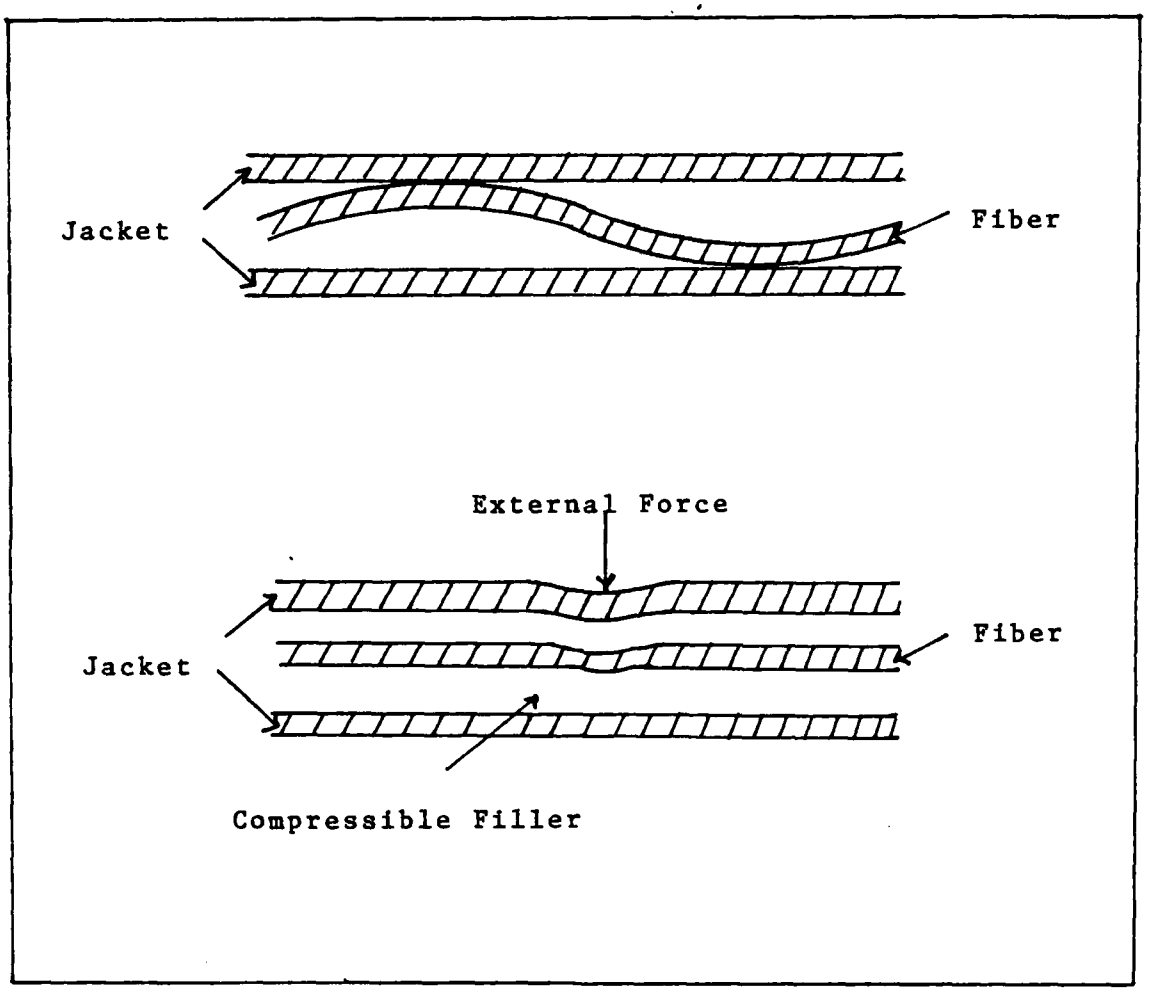

(11:57)

Figure 9. Fiber Microbends.

cladding and create a power loss.

The major factor that limits the bandwidth of optical fibers is intermodal distortion. The higher order modes that propagate in a fiber have lower power content but they also take longer to traverse the length of the fiber. When the optical signal reaches the termination of the fiber the higher order modes, carrying the same information, arrive later, thus interfering with the lower order modes of subsequent information signals. Obviously, the longer the fiber, the greater the time spread between the higher and lower order modes and the greater the distortion. Therefore, fibers that support more modes have greater bandwidth limitations and the units of this type of distortion is measured in Hertz per meter.

While surveying for optic fibers to be used on this system all types of fibers were considered initially. However, single mode fibers were omitted from consideration because of cost. Table V lists the parameters of four different fibers which represents a fair cross section of commercially available fibers and fiber cables.

Emitters, Detectors and Connectors

Emitters, detectors and connectors will be discussed in most general terms because for the purpose of establishing this system any optical power source or photodetector with equivalent electrical characteristics as the SPX 1775 and SPX 1777 could be used as long as they are designed for single

Table V

Optical Fiber Comparison

Parameter	Manufacturer			
	Corning	Augat	ITT	Belden
Core radius (μm)	85	250	50	50
Numeric aperture	0.26	0.4	0.2	0.2
Bandwidth (MHz/Km @ 850nm	100-300	5	200	400
Loss (dB/Km)	3.2-4.0	37	3	3
Price ($/m)	Not available	1.65	.60	1.66
Jacketed	No	Yes	No	Yes
Available at AFIT	No	No	Yes	No

strand fibers instead of multistrand bundles. Connectors need only be able to couple the fiber to the source or detector with good repeatability in mechanical alignments.

Optical power sources are generally classified into two categories, Light Emitting Diodes and Laser Diodes. Laser diodes are normally used for very long communications links because of their highly directional, higher output power levels and very short time constants. Laser diodes can be modulated up to the Gigahertz range and higher; however, for this greatly improved efficiency, their cost is proportionally higher than the more contemporary LED's.

Typical output power levels for LED's are in the microwatt to milliwatt range, and rise times of 10 to 50ns. If a maximum of one third of the pulse duration is allowed for the rise time, the bandwidth is limited to approximately 30MHZ.

Light Emitting Diodes normally come in one of two standard packages known as surface emitters or edge emitters. Surface emitting LED's are permanently connected to a fiber with an epoxied butt joint right to the active surface of the diode. Edge emitting diodes have internal reflecting plates that direct the output optical power parallel to the active area creating a directionalized radiance pattern. This allows more power to be coupled to a fiber that is not butted directly against the diode's surface.

Surface emitting LED's come with a pigtail fiber permanently attached to the diode and the communications fiber

Table VIII

Equipment Required

Description	Quantity
LED	4
PD	4
Panel mount BNC mating connector	12
SMA Fiber terminating connector	2
DPDT Switch	12
Front panel	4
Optical fiber	As Needed

Table IX

Support Equipment Required

Soldering iron and solder	Optical power meter
Wire wrap tool	HeNe Laser
Signal generator	Fiber holding fixture
Oscilloscope	Fiber termination kit

terminated with a standard SMA style connector can be tested with this system. Since one CMTU and three MTU's are available, four such systems could be constructed.

System operations tests will consist of a complete functional check, and an LED emission pattern characterization. Also, when the fiber to be used is terminated with a connector it will be tested for proper termination, numeric aperture and fiber attenuation.

An Operations Manual will be prepared for the complete system. The manual will contain a functional description of the system and its subsystems, instructions for front panel operation and schematics of all components in use within the units.

Material Required

Table VIII lists the equipment that has been procured, either locally (in-house), or commercially purchased, to complete this work.

Support Equipment

Table IX lists the support equipment required.

Additional Support Required

The only additional support required is a minimal amount of machine shop support in making new front panels for the CMTU and MTU cabinets.

Carrier modulation is possible on an internally generated 20MHz clock signal or on an externally provided carrier signal.

- The CMTU and MTU's received from Spectronics are very similar in design and construction. The difference in the units lies in their control logic circuits and their interface with their test sets. Because of their similarities, their changes are identical and are as follows.

** Have new front panel made.

** Mount new LED, PD, BNC connectors and function control switches.

** Remove internal control circuitry and cross connect wiring.

** Design, construct and install new control circuit that will implement the selected functions of baseband transmission or carrier modulation. Install new cross connect wiring for front panel controls and data lines to and from the LED driver card and post detector amplifier.

As a result of these changes the system is now a simplex, single strand, fiber optics communications system capable of transmitting both digital baseband and carrier modulated signals. The system is self contained with both the transmitting LED and receiving PD housed in the same cabinet. The system is compatible with any TTL, digital modulating system for creating PCM, PPM, PDM or quantized PAM baseband signals. The fiber link in use during test is looped from the LED to the PD on the unit in test. Any optical fiber

Table VII

Augat 698-069DG1

Description:	p-i-n Photodiode Coaxial package
Active area	0.105 X 0.043 in.

Optical/Electrical Specifications @ 25°C, V_{cc} = 5.0V

	Min	Max	Typical
Reverse voltage			100V
Dark leakage current @ V_{bias} = 50V			20na
Capacitance @ V_{bias} = 5V			18pF
Responsivity @ 880nm			0.53A/W
Response time @ V_{bias} = 50V			3.8ns
N.E.P. @ V_{bias} = 50V, @ 1KHz			10^{-13} W/Hz$^{1/2}$

(20)

Table VI

Augat 698-013EG2

Description:	Edge Emitting LED		
Optical/Electrical Specifications @ 25°C and V_{cc} = 5.0V			
	Min	Max	Typical
Reverse breakdown voltage	3.0V		
Forward voltage @ I_F = 100ma		1.9V	1.75V
τ_p			880nm
$\Delta\tau$			40nm
Power output			38μW
Optical rise and fall time			20ns

(20)

is not being used.

- The Spectronics SPX 1775 LED is being removed for two reasons. First, it was initially designed for use with multistrand bundles as evidenced by the description of its emission pattern in Chapter 2. Second, the connecting bracket manufactured by Cannon Electric Division is not suited for a simplex system where frequent changing of the optical fiber is expected. This original bracket, which houses both the LED and the PD, is being swapped out for a more conventional SMA coupling mount. The LED selected as the replacement is the Augat 698-013EG2. The pertinent optical and electrical specifications are listed in Table VI. This LED is bulkhead mountable and has equivalent characteristics as the SPX 1775.

- The Spectronics SPX 1777 PD is being removed because of its mounting bracket and its suspected age. The detector is being replaced with an Augat 698-069DG1. This new detector is also bulkhead mountable with an SMA style mating connection. Specifications for this detector are listed in Table VII. A quick comparison with the information listed for the SPX 1777 shows that they are equivalent.

- The CMTU Test Set from the data bus package is not being used because of its inherent dependency on control logic with the CMTU. The system that has been designed is very basic, and is composed of an optical transmitter and receiver housed in the same cabinet, and the fiber link. Inputs are available for transmitting digital baseband signals.

Lastly, an Operations Manual was prepared to facilitate future use of the system.

Approach

The most effective use of the available equipment was the primary concern throughout this work. The Spectronics EMI/EMP Resistant Data Bus has been determined to be capable of supporting a single strand fiber optics communications system with several modifications. The changes and the reasons for these changes are as follows.

- The Valtec multi-strand fiber cables needed to be replaced with single strand optical fiber. The ITT fiber that was already available was terminated with standard SMA style connectors as described in Chapter 2. Because the fiber was not jacketed, there was a slight modification to the termination. The crimp sleeve which would normally be clamped to the jacket was omitted. The rest of the termination procedure of epoxying and lapping the face of the connector and fiber was completed as per manufacturer's directions. The connector selected for use was the Optical Fiber Technologies, Inc., part number 252-S-A. This connector is suitable for fibers with core diameters less than 125μm and has a connection loss of less than 2dB.

- This optical fiber system is initially being designed as a simplex system with information flowing in one direction from a single transmitter to a single receiver. Therefore, the radial coupler that accompanied the Spectronics Data Bus

III. Problem Statement and Approach

This chapter contains the exact problem statement of this work, its scope, the approach to the problem and lists the material and equipment required to complete the task.

Problem

Design and implement a single strand fiber optics communications system to be used by AFIT faculty and students for future communications experiments and research.

Scope

The bulk of the background investigation for this work was done in the area of optical fibers and their use as a communications media. Secondary to this was research into optical sources, photodetectors, optical fiber connectors and couplers, with emphasis on their applicability towards this work.

A survey of both on-hand equipment and commercially available equipment was conducted to determine the most effective use of resources.

In-house available equipment deemed necessary was then assembled along with commercially purchased items to construct the system. Once the modifications on existing equipment and construction of new components were completed, operational tests on the equipment were performed. Operational tests were done at both the component and the system level.

If a ray enters the fiber at some angle θ, is trapped and propagates down the fiber it maintains the same angle with respect to the core axis until it reaches the other end of the fiber. Therefore, when the ray exits the fiber, it does so at the same angle at which it entered. The angle of the expanding exit beam is the same as that of the light ray that was accepted at the entrance to the fiber, and this is the numeric aperture.

The last test is that of determining the attenuation of the fiber. This is the simplest of the four where the fiber is connected to an optical power source and a power reading is taken from the other end of the fiber with an optical power meter. Then the fiber is shortened and another power reading is taken. The difference in power readings divided by the length that the fiber was shortened yields the fiber's attenuation constant in units of decibels per meter.

For a fiber optic communications system without splices or fiber to fiber connections these four tests give sufficient information to perform power budget calculations for the optics medium. When the responsivity of the photodetector is known along with the output power of the LED, it can be determined if enough power will be coupled to the fiber and whether the fiber will attenuate the optical signal beyond the capabilities of the detector.

used to determine if the optical source is suitable for the desired purpose.

Fiber termination characterization is really just a simple check to see how well the fiber face has been prepared. The terminated fiber end under test is attached to a compatible optical source with the other end of the fiber connected to an optical power meter. An initial reading is recorded; then the fiber is rotated 90° three times with readings recorded at each of the positions. A comparison of the readings will give an indication of whether the face of the fiber has been finished flat and normal to the axis of the fiber.

The optical power source normally used to measure the numeric aperture (NA) of a fiber is a low powered laser instead of an LED. The laser beam is focused on the end of the fiber and the other end of the fiber is aimed at a screen located a convenient distance away. A simple measurement of the beam image on the screen is taken, and knowing the distance of the screen from the fiber end the beam angle can be calculated by taking the arctangent of the beam width on the screen divided by twice the distance from the fiber end to the screen. A fiber's numeric aperture is a measure of its light collecting ability and is defined as the sine of the maximum angle that light can enter the fiber's face and be trapped by internal reflections inside the fiber's core. This test is a valid method of determining a fiber's NA and can easily be proven by using simple geometric ray optics.

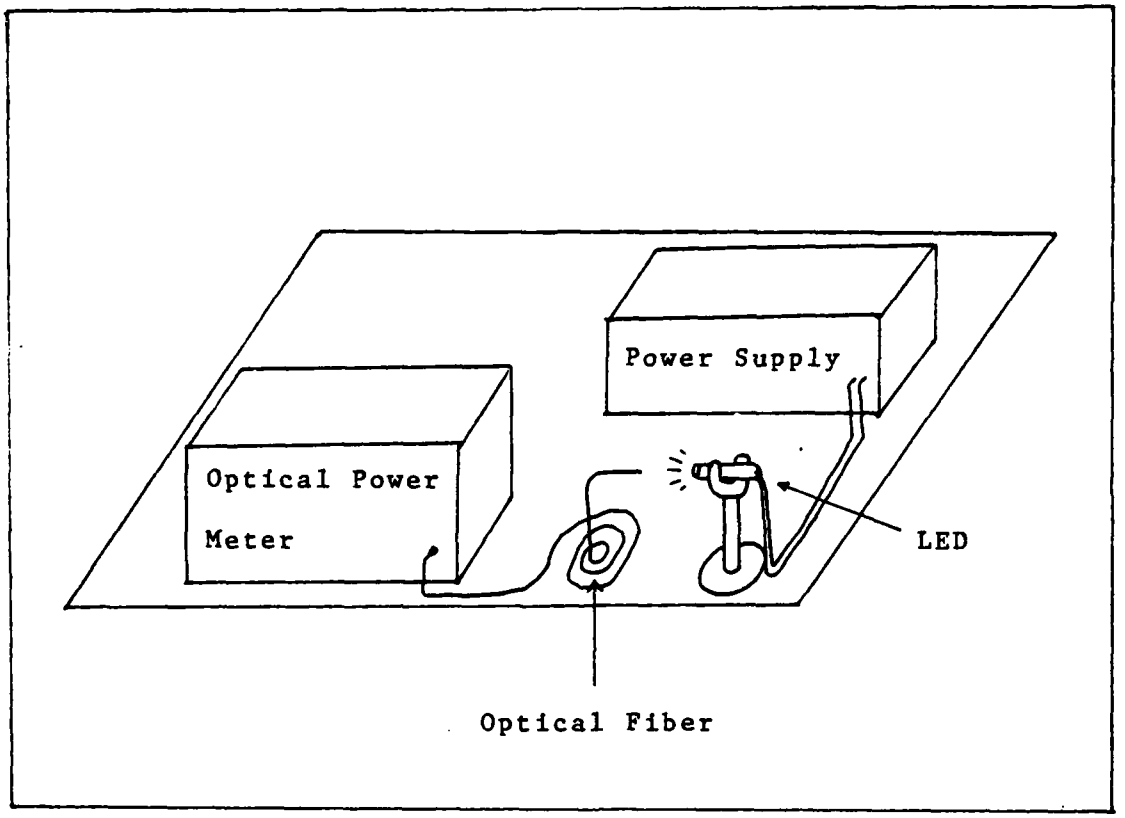

Figure 11. Setup for Measuring LED Emission Pattern.

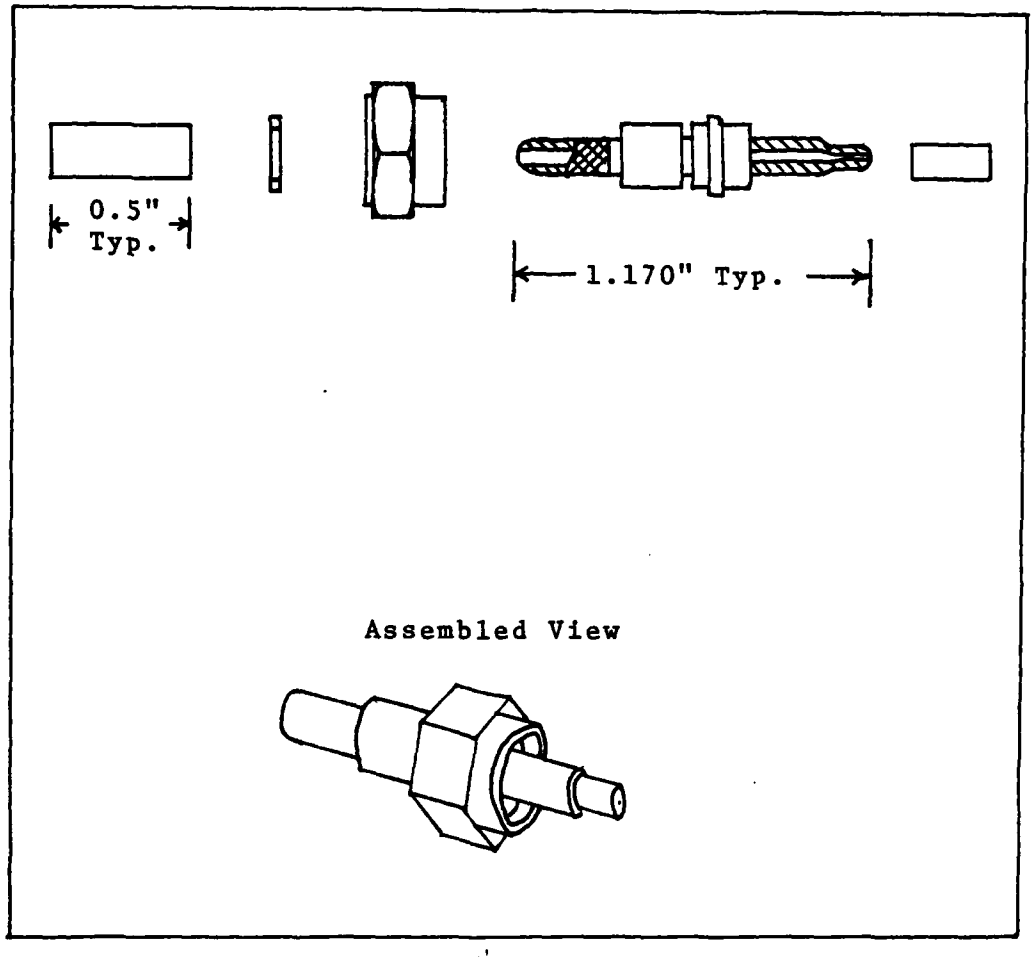

(7)

Figure 10. Optical Fiber Technologies, Inc., 200-S Styled SMA Connector.

Figure 10. These connectors are moderately priced and readily abailable in sizes to fit standard fiber core diameters.

These SMA connectors are of the concentric-sleeve type as opposed to the tapered sleeve or V-groove types. Also, they have no lens systems for beam expansion nor index matching fluid to increase coupling efficiency. They are simple dry joint butt connectors.

Experimental Measurements of the Optical System

There are four very basic measurements that can be performed on an optical fiber communications system that yield somewhat of an overall characterization of the optical link. These tests are: optical source output radiation pattern, fiber termination characteristics, numeric aperture of the fiber and fiber attenuation. A general description of these tests will be presented in this section.

To determine the emission pattern of the optical source, the source must first be firmly fixed in a position which allows access to the output energy from all directions. Such a position is depicted in Figure 11. A short piece of optical fiber will serve as a light collecting instrument which is connected to an optical power meter. The relative power readings are recorded as the fiber is moved around a hemispherical surface insuring that the polished face of the fiber always remains normal to the light source. The power measurements can then be plotted and a diagram of the output emission pattern is obtained. This information can then be

must then be spliced or in some way connected to the pigtail. This method may be adequate for fixed communications links, but the edge emitting LED is more suited for a system where the fiber link might be disconnected and reassembled many times. Edge emitting LED's are available packaged in bracket or bulkhead mountings complete with microlens systems for additional focusing of the optical power allowing better coupling efficiency to the fiber.

Photodiodes use the photoelectric effect of semiconductors to convert optical power to electrical current. The p-i-n PD is used as a simple photon counter which outputs a current proportional to the number of photons impinging on its active surface area. The avalanche photodiode is similar in that its active surface area creates an electron flow when photons strike, but as the electrons propagate through the semiconductor they cause additional electrons to move giving the device a relative gain in output current. The avalanche PD's are used when there are low input optical power levels requiring a more sensitive optical receiver.

Photodetectors used in fiber optic communications systems are available packaged in all the standard mountings with standard fiber coupling connectors.

Optical fiber connections range from arc fusion welding of the glass to temporary plastic clip-on connectors. By far the most common type connector for a reliable, removeable connection is the standard SMA styled metal screw-on fiber connector. An example of this type of connector is shown in

IV. System Implementation

The eight station, Spectronics EMI/EMP Resistant Data Bus was converted to a two piece, single strand optical fiber communications system after the changes described in the third section of Chapter III. The changes were accomplished in four phases. Chronologically, the CMTU and MTU cabinets were stripped of wiring and components not needed in the new system. A new controlling circuit was designed and built to accomodate the functions of the new system. The cabinets were modified to properly house the new components, connectors and switches. And finally, the components were installed on the modified cabinet and the test fiber was terminated with new connectors. Details of each of these four phases are presented in the following four sections.

Component Removal

It was determined that five of the nine circuit cards in the CMTU and MTU would be used in the new system. These five were circuit cards A5 through A9, namely the ECL/TTL Convertor, ECL Sync Detector, LED Driver, Preamp and Postamp Signal Conditioning cards. The last three of these cards listed above were kept to provide the TTL interface to the LED and PD. The ECL Sync Detector also generates the system clock signals of 100MHz, 20MHz and 4MHz. The ECL/TTL Convertor card was kept to provide TTL compatible clock signals that could be used as digital carrier signals for the system.

The remaining four cards were not discarded entirely. The A4 card was stripped of all wiring and components to be used for the new controlling circuit. The integrated circuit chips on the cards A1 through A4 were then available for use in this new circuit. All cross connect wiring was removed from the card sockets and front panel. However, the power supply and serial data stream lines were left intact.

The LED and PD connector was removed and then it was determined that the front panel should be replaced because of the numerous holes that would remain unused with the new system.

Control Circuit Design and Construction

The control circuit that was designed was done so to properly handle the functions described in Chapter 3. On the transmit side, either baseband or externally modulated carrier TTL signals were coupled directly to the LED driver circuit. Also when so desired, the input baseband signal modulated either the internal 20MHz carrier or an externally provided carrier. On the receive side, the circuit had to do the inverse of the transmit. Namely, it had to couple a baseband signal directly to the output, or if carrier modulation was used then it had to regenerate the original baseband signal.

Figure 12 is a logic diagram of the circuit designed. In this figure the symbols are as follows: S1, S2 and S3 are controlling switches, BBI is baseband input, BBO is the

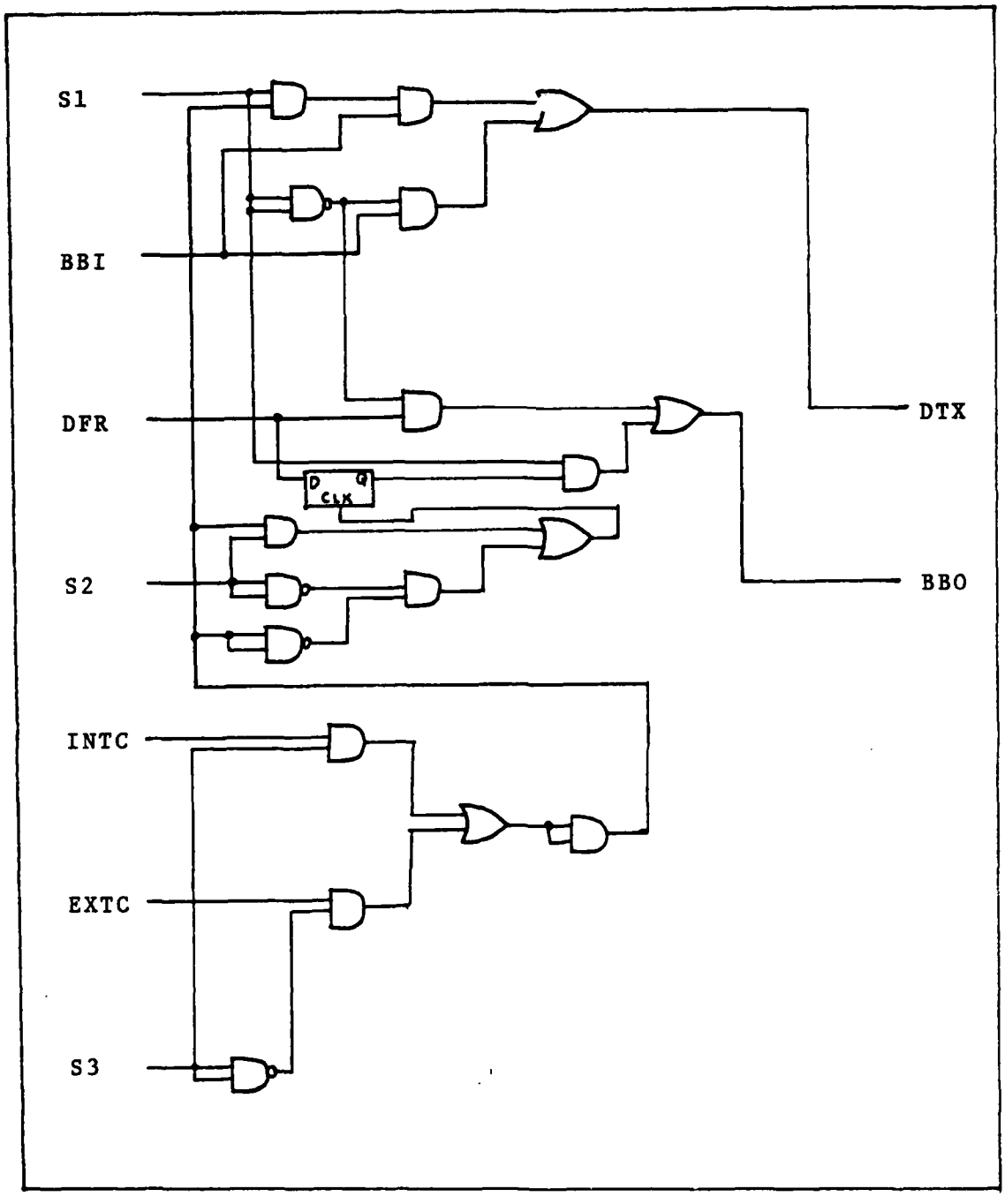

Figure 12. Logic Diagram of Control Circuit.

baseband output, DFR is data from the receiver, DTX is data to transmitter, and INTC and EXTC are the internal and external carriers respectively.

When S1 is low, BBI and DFR are connected to DTX and BBO simultaneously. This state constitutes baseband transmission mode only. When S1 is high, the carrier signal selected by S3 is AND'd with BBI creating the carrier modulated signal to DTX. Also, when S1 is high, the received modulated signal, DFR, is the input to a D flip-flop which is clocked by either the carrier or the inverted carrier (selected by S2). The D flip-flop is triggered by the positive going transition of the of the carrier frequency and therefore remains high through the entire period of the carrier signal. This function demodulates the signal back to baseband and S2 performs the function of a synchronizer. There is no actual synchronization performed here but when the same carrier frequency is used for both the transmit and receive the transmission delay could cause the signal to be sampled during the low state of the received carrier modulated signal. If this occurs then the output to BBO will always remain low. When this happens, changing the sense of S2 effectively causes a 180° shift in the carrier triggering signal resulting in proper sampling timing.

This circuit was assembled on the empty A4 card using standard wire wrap techniques. The wiring diagram for this circuit is given in Figure 13. After its construction, the circuit was tested and all functions operated as designed.

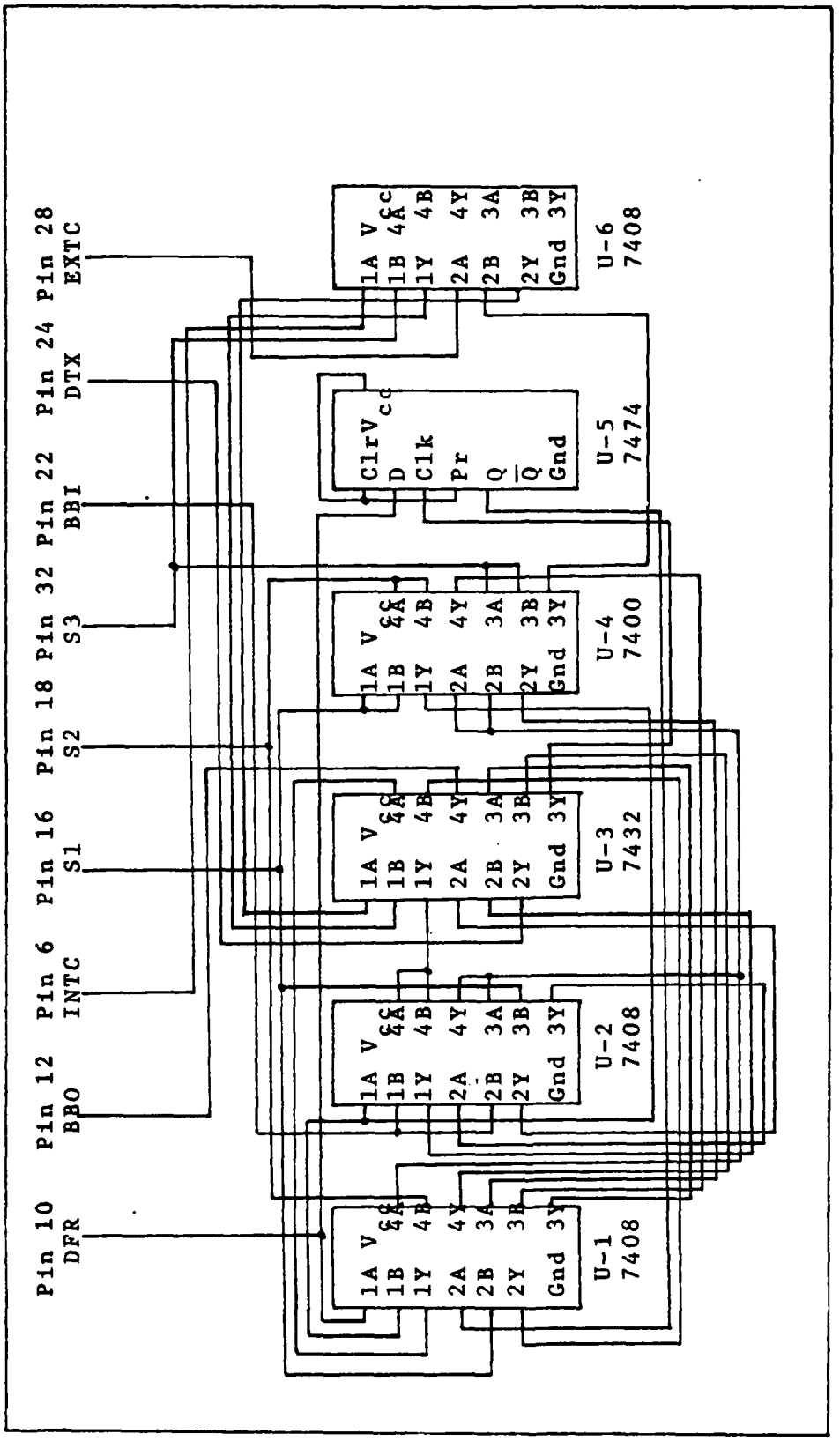

Figure 13. Wiring Diagram of Control Circuit.

Cabinet Modifications

Changes in the cabinets of the CMTU and MTU were very similar. The only difference was that with the MTU three BNC connectors were removed from the rear panel to be installed on the front. The two common changes were the design and acquisition of a new front panel and removal of an alignment flange.

The RFI enclosure for the LED driver, preamp and signal conditioning cards had an alignment flange for the LED and PD mounting bracket. The flange protruded through the front panel to the bracket and ensured proper alignment of the LED and PD to the driver and preamp for a direct connection. This flange was removed entirely but the RFI enclosure was retained as a circuit board mount for the three cards within.

The front panels that came with the original equipment could have served with the new system with all the existing holes covered with small plates. This, however, would have necessitated moving the RFI enclosure and making new holes for the new LED and PD. Also, the front panel was etched and painted describing the function of the connectors and switches. Since all connectors were to serve new functions and more switches were to be added, the panel labeling would have been misleading. Therefore, a new panel was designed and ordered through the machine shop. The original schematic for the front panel was used as a guide and a description of the new panel is given in Figure 14.

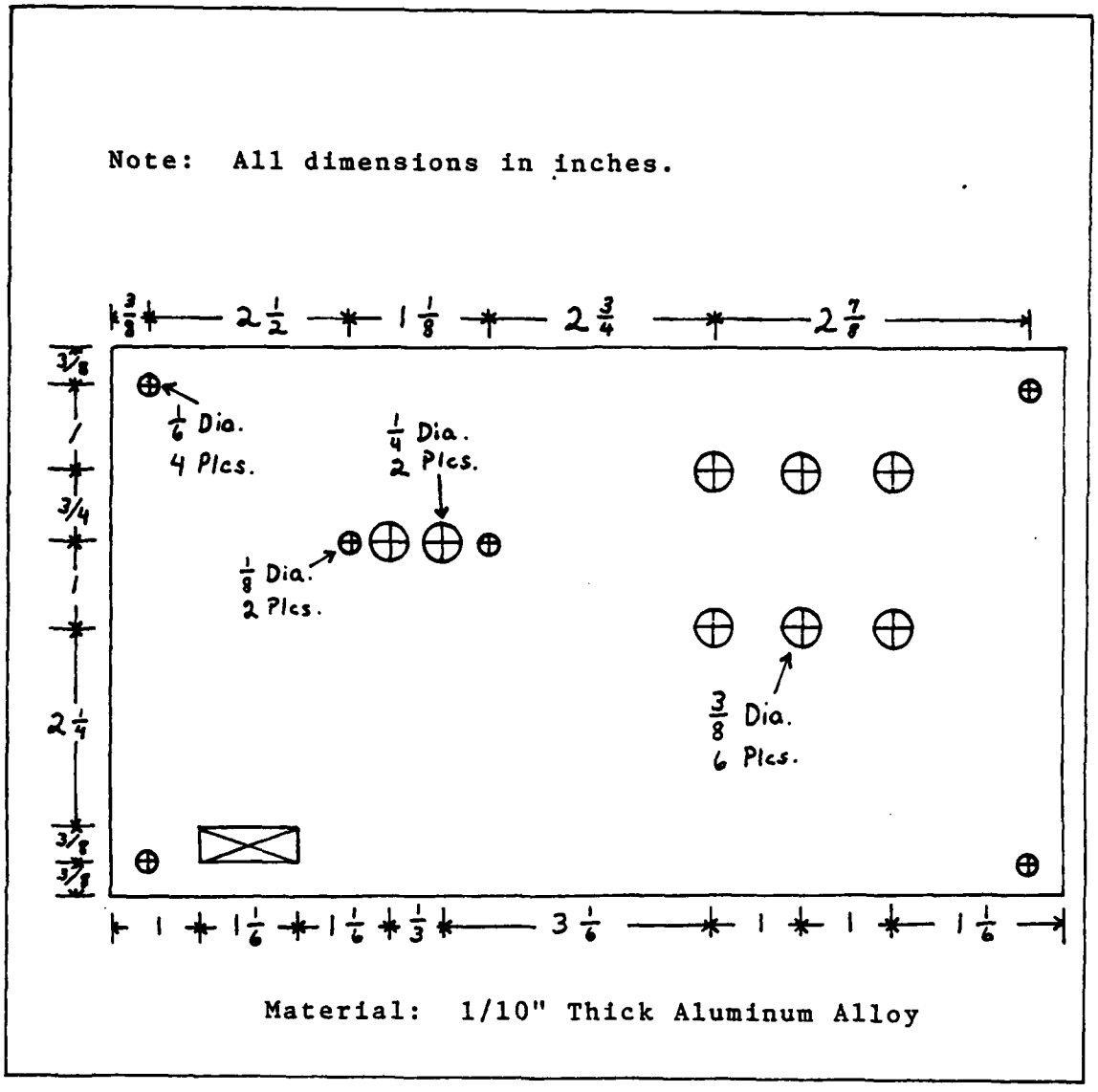

Figure 14. Diagram of New Front Panel.

Component Installation and Fiber Terminations

When the Augat LED's and PD's were received, they were installed and soldered to the driver and post detection amplifier cards with only one minor problem. The mounting holes bored in the new front cover were aligned with the positions of the old LED and PD, and the resulting dimensions did not allow room for the locking nuts or the hex nut locking clamp for the fiber connectors. Therefore, the two mounting holes were filed out to make a rectangular opening large enough to accomodate the new components and a small cover plate with properly aligned mounting holes was made to hold the LED and PD. This solution has proven to be quite adequate.

In the Spectronics Technical Report on the EMI/EMP Resistant Data Bus, much effort was dedicated to the description and design of the post detection amplifier and signal conditioning circuit cards. Primary in their concerns was the upper cutoff frequency of these components in conjunction with the photodetector. In their analysis, the upper limit for the system rise time was determined to be 35 nsec. Leaving approximately the same time period for the fall time, the system bit rate was thus limited to 12.5 MHz. Because of a delay in receiving the LED and PD for this work, ample time was available to investigate these frequency limitations. To simulate the completed system equivalent LED's and PD's were connected to the system via long wires and mounted on a

temporary mounting board. This was necessary because the components were not of the SMA compatible, bulkhead mounting types. This did, however, allow very convenient test points for monitoring circuit response. It was noted that as the frequency of the transmitted signal was increased the output of the postdetection amplifier went from a near perfect square wave to a triangular waveshape of changing slope nearly proportional to the input frequency. The slope of this signal approached zero as the frequency reached 10.5 MHz. More importantly, however, was the fact that the average level of this triangular waveshape varied with input optical power levels. This directly effected the frequency limitations of the system. If the optical power was great enough, the signal never fell below the threshold of the post detection amplifier and the system output remained high. If the optical power was too low then the peak of the triangular wave never exceeded the threshold and the output remained low. At lower frequencies, below 1 MHz, this effect was negligible. No optical power measurements were taken at this time because of the impending LED, PD and optical fiber changes.

All tools and materials required to attach the stainless steel OFTI, SMA styled fiber connectors were located in the new Engineering Optics Lab located in building 194, Area B, of Wright-Patterson AFB. Using an optical fiber stripping tool, enough of the plastic coating was removed from the ITT fiber to allow just the core and cladding to extend approxi-

mately a quarter of an inch through the alignment hole of the connector. Epoxy was then mixed and applied to the fiber and connector. To insure adequate adhesion, the back of the connector was filled with epoxy along with a small bead of epoxy on the connector's face. The fiber was moved in and out of the connector a few times to allow the epoxy to completely fill the fiber alignment cylinder. The epoxy was cured with a heat gun for approximately ten minutes, until the epoxy turned a very dark red, and then the excess fiber protruding through the epoxy bead on the face of the connector was broken off. The excess epoxy and fiber on the face of the connector was removed with a coarse lapping film and the connector's face and fiber end was then polished flat with finer grades of lapping film. This procedure was used on both ends of the optical fiber and continuity was checked by placing one end of the fiber in front of an incandescent light bulb and checking the other end of the fiber under a microscope. No problems were encountered while making this two meter piece of test fiber.

V. Fiber Testing and System Operation

The testing done on the completed system as described in the previous chapters can be broken down into three categories. First, the fiber itself was tested for Numeric Aperture, attenuation, and connector loss. Next, the LED was energized and its emission radiation pattern was characterized. And last, the system was tested for both its modulation capabilities and frequency response. The following is a description of the tests and their results in the order presented above.

Fiber Tests

Numeric Aperture. The test performed to measure the fiber's numeric aperture (NA) was both the most involved and the most interesting of the three tests done on the fiber. The NA test was performed on the fiber before the OFTI connectors were installed on the ends. This procedure, without connectors, necessitated that the fiber ends be cleaved to obtain a flat face perpindicular to the fiber axis. The XYZ positioning clamp to hold the fiber at the focal point of the laser light also required that about three inches of the plastic coating be removed. This was quite difficult because the fragile glass fiber inside broke repeatedly. Table X lists the equipment required for this test.

Table X

Equipment Required for NA Test
1 mW HeNe Laser Light Source
Focusing lens
XYZ Positioning Clamp
Fiber stripping tool
Etching tool
Adhesive tape
Microscope
Projection Screen

The procedure for the NA Test is as follows:

1. Strip off protective plastic coatings from both ends of the fiber under test. (In this case, one end needed three inches of fiber exposed so the fiber would fit properly into the positioning clamp.)
2. Cleave each end of the fiber as close as possible to end. The cleaving procedure used was to tape the extreme end of the exposed fiber to the working surface, then with the aid of the microscope, carefully etch the glass with the etching tool, then while holding the taped end of the fiber firmly with one hand slowly pull the other end of the fiber. A good

cleave is achieved when the fiber breaks at the point of the etch mark. The fiber end should now be completely flat and perpendicular to the fiber axis.

3. Place the fiber so that one end is in the XYZ Clamp and the other is fixed in a position normal to and a convenient distance away from the projection screen. (In this case a piece of clean white paper was used as the screen.)
4. Turn on the laser light source, and with the XYZ Positioning Clamp, move the cleaved fiber end to the focal point of the lens in front of the laser. (When the fiber end is at the focal point, the optical power exiting the other end is at a maximum.)
5. Measure the diameter of the circle of light on the screen, "d", then measure the distance from the fiber end to the screen "l".

The data from these two measurements are then used in the equation $NA = \sin[\tan^{-1}(d/21)]$ to determine the fiber's numeric aperture.

When this test was performed on the ITT fiber, the diameter of the light circle was 4.5 inches, and the distance from the screen to the fiber end was 12 inches. These measurements resulted in a calculated NA of 0.184 which correlates very well with the stated NA of 0.19 from the manufacturer.

One very important property of optical fibers must be kept in mind before performing this test. When light is

initially launched into a fiber, many modes will propagate for a short distance before the higher order modes radiate away through the cladding. Therefore, to measure the "equilibrium NA" versus the "insertion NA", a piece of fiber in excess of 10 meters in length should be used or some other type of mode stripping would have to be accomplished. One common form of mode stripping is to remove any protective coverings from the fiber and directly expose the core, if possible. Then, while bending the fiber at the exposed section, cover the glass with an index matching liquid like glycerin. The number of modes that can be removed utilizing this technique is directly dependent on the radius of curvature at the bend, and the index of refraction and purity of the index matching fluid.

In the case of this work, the length of fiber used for this NA test was approximately 100 meters. Therefore, the 0.184 NA calculated is assumed to be the equilibrium NA.

Other noteworthy observations resulting from this test involve the shapes of the light images on the screen while trying to get a good cleave on the fiber end. In particular, there were three different times that it was thought that there was a good cleave on the end of the fiber, but the image on the screen was not even close to the expected perfect circle.

A good cleave was achieved on one end and was installed in the XYZ clamp. The other end was cleaved and under the microscope it appeared to be a good finish. However, while

the baseband signal only.

The last test performed on this single strand fiber-optic communications system was that of average optical power output versus frequency. The results of this test should be helpful when system optical power budget calculations are made. The Photodyne Optical Power Meter was used with the fiber constructed for this work to record the power levels. The measured fiber loss of 9.4 dBm was added to each reading to give the actual power output of the LED at each frequency. Figure 17 is a plot of the results of this test. It was noted that at 22 Mbit/sec there was a rise in power of 0.5 dBm and this was also the cutoff frequency for the photodetector conditioning circuit. Therefore, it was presumed that this optical power level of 2.3 dBm was also the upper threshold of the receiving circuitry.

The output power was also checked at dc, and a level of 2.8 dBm was observed. This is identical to the power level transmitted at frequencies above 32 Mbit/sec which confirms that the LED remains on constantly above this upper bound.

electro-optic interface. When the signal from the LED driver was checked it was observed that at 32 Mbit/sec the driver output remained high constantly. Additionally, when the output of the post detection amplifier was monitored it was observed that the signal level remained sufficiently high enough to stay above threshold at rates higher than 22 Mbit/sec. Hence this 22 Mbit/sec upper bound was real and determined to be the result of the relatively slow time constant of the circuit comprised of the PD, post detection amplifier, and signal conditioning cards. At this point it was also determined that the internal 20 MHz (40 Mbit/sec) carrier could not have been transmitted as believed in previous tests. When the carrier signal was modulated by the baseband, it merely kept the LED activated until the baseband signal returned to the low state and therefore the actual signal being transmitted optically was identical to the baseband only input.

For the externally provided carrier mode the carrier frequencies enjoyed the same range as the baseband mode. Carrier frequencies from 160 Kbit/sec to 20 Mbit/sec were used on a range of baseband signals from 80 Kbit/sec to 10 Mbit/sec. It was noted that in this mode the limitations were caused by and responded identically to those in the baseband mode. That is, when baseband signals below 80 Kbit/sec were used, regardless of the external carrier frequency, the duty period of the square wave dropped below 40%. An if the carrier frequency was set above 22 Mbit/sec the optical signal followed

was actually taking place. To test for proper operation, the external carrier modulation mode was used but with the speeds of the baseband and carrier reversed. In this configuration it was very evident that the baseband of 2 Mbit/sec was being turned on and off at the carrier rate of 200 Kbit/sec and operating as designed. Without a hardware change it was impossible to perform the same test using the internally provided carrier. Up to this point it was thought that the internal carrier mode also functioned as designed.

Next, the range of the system was tested. Initially, it was checked only in the baseband mode starting with a bit rate of 200 Kbit/sec. While dropping the bit rates, at 80 Kbit/sec there started a noticeable change in the duty period of the square wave at the output. At this bit rate the duty period had dropped to about 40% instead of the expected 50%. By the time the bit rate was dropped to 40 Kbit/sec the duty period had dropped an additional 30%. Therefore, it was deemed that the low end of the input range on the system was 80 Kbit/sec. On the high end a usable signal was still present at 22 Mbit/sec. However, the output of the function generator at this speed had noticeable roll-off and ringing, because of this imperfect input signal and it was impossible to determine if the system could reliably operate at higher speeds. Since the system did operate well up to this speed the input bandwith was limited from 80 Kbit/sec to 20 Mbit/sec.

This upper bound of 20 Mbit/sec was investigated further by removing the front panel to check signal levels at the

input baseband frequency of 100 KHz.

The system functional tests consisted of transmitting four types of signals across the optical path. The four types were; straight baseband, externally modulated baseband, and internally modulated signals using both the internal 20 MHz carrier and an externally provided carrier. Two Wave-Tech function generators provided the signals for both the baseband and external carrier. A dual trace Hewlett-Packard oscilloscope was used as the receiving equipment. The oscilloscope's fastest scan time was 25 nsec/div with a grid size of 10 divisions and was adequate for displaying signals up to 20 MHz. The function generators had both variably attenuated outputs with a choice of waveshapes and a TTL compatible synchronous pulse output. The TTL outputs became considerably distorted past the speed of about 2 MHz and therefore, the waveshape function outputs were used exclusively during testing. This choice brought about a nuisance problem in that this output was not linear and every time the output frequency was changed the amplitude and dc offset of the signal had to be adjusted.

System functional tests were completed in two stages. First, all four functions were checked with a continuous bit stream at the rate of 200 Kbit/sec for the baseband and an external carrier continuous bit stream of 2 Mbit/sec. Then the speed ranges of the four functions were determined.

All four functions performed as expected. However, since the system only outputs a baseband signal when it is in the carrier mode it was impossible to see if the modulation

the Full Width Half Max angle of this LED was about 6°, or from -3° to +3°. This result confirms the high directionality of the edge emitting LED. However, it must be kept in mind that the LED comes housed in a SMA compatible mounting and the actual emission source is recessed 3/8 inches inside the mounting and this effects the radiation pattern at distance greater than this.

System Operational Tests

Operational testing was rather limited for the optical communications system constructed in this work. It was limited inasmuch as signal to noise and bit error rate tests were not performed. Functional tests for both baseband and carrier modulation as well as average output optical power versus frequency of baseband input were performed.

Before the functional and frequency response tests were performed, an attempt was made to determine the absolute loss of the fiber constructed for this project. The Photodyne Optical Power Meter was first placed directly in front of the SMA mounting of the LED and a reading of 0.4 dBm was recorded; then the fiber with connectors attached was placed between the LED and the power meter and a reading of -9.0 dBm was observed. This 9.4 dBm, or 88.5%, power loss was the absolute loss of the fiber media, however, it was impossible to determine how much loss could be contributed to the fiber characteristics or the connections themselves. This test was conducted on the system in its completed configuration with an

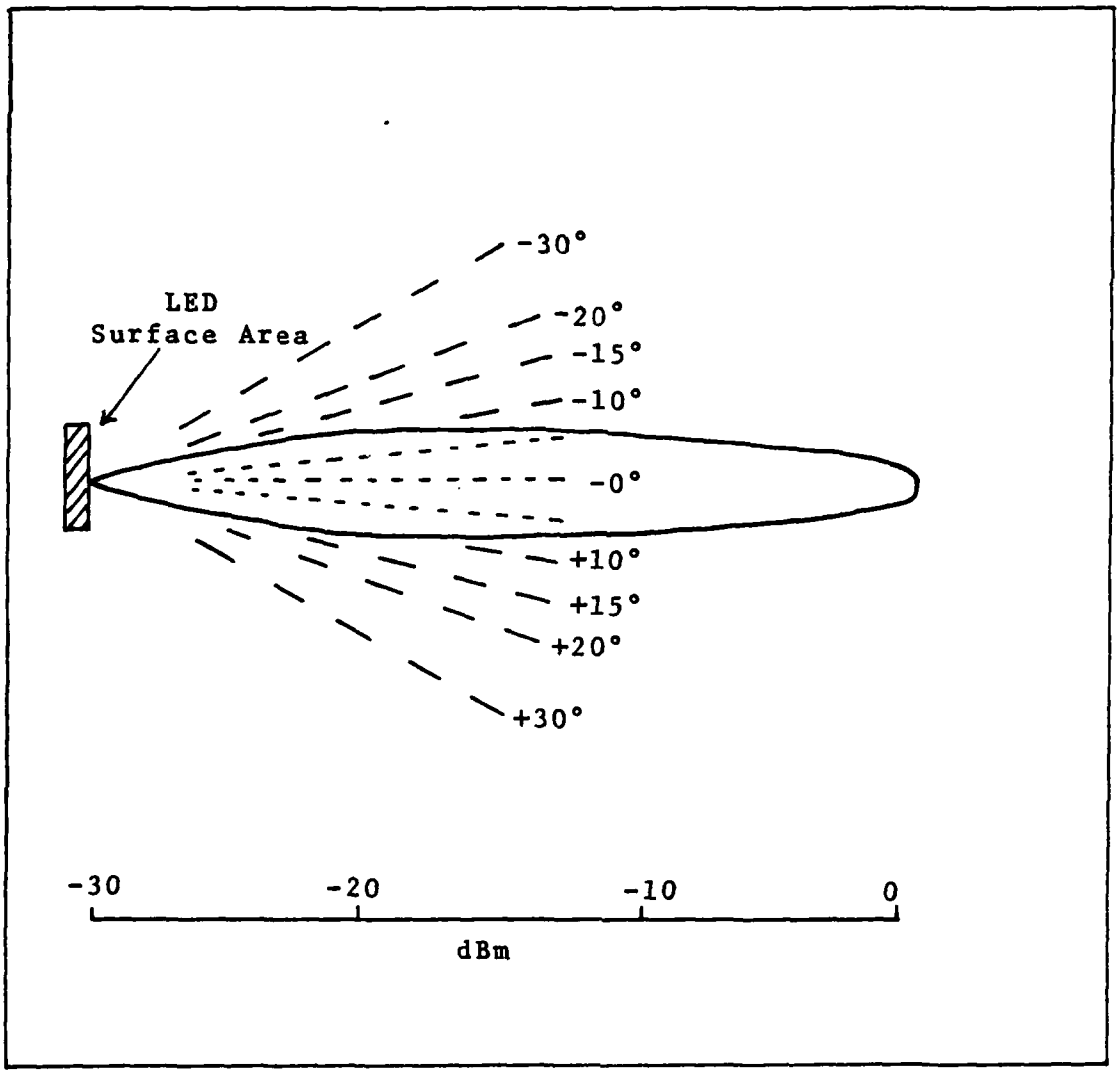

Figure 16. LED Emission Radiation Pattern.

connector placed on and parallel to the grid, the light collector would remain in the same plane as the emission angle was swept. Since this test was one of relative measurements, one main concern was to keep the light collector the same distance from the source and the actual distance between the collector and source was insignificant as long as the optical power was within the range of the meter. A distance of approximately three inches was used for this test. The data collected from this test is listed in Table XII.

Table XII

Emission Radiation Pattern	
Angle from LED Axis	Relative Power Reading
-15°	-29 dBm
-10°	-19 dBm
-5°	-9 dBm
0°	0 dBm
+5°	-9 dBm
+10°	-19 dBm
+15°	-29 dBm

The plot of this radiation pattern is shown in Figure 16. From this data one could extrapolate to determine that

in this type of test it is impossible to determine if the loss was caused by axial displacement or angular misalignment. Also, there are uncontrollable nonlinearities in the connector, LED, power meter. That is to say that even though the locking clamp of the connector was not moved there does exist some limited amount of play in the connector and this may be the cause of the axial displacement loss rather than the positioning of the fiber concentrically within the alignment cylinder.

Because of the nature of this work these results are relatively insignificant. However, when the power budget formulas for an optical power link are solved the difference in positioning of the fiber connectors may become a very significant factor. This test allows the designer of a system to know the range of the controllable factors he has to work with.

LED Emission Radiation Pattern

The emission radiation pattern of the Augat 698-013EG2 LED was determined after it was installed in the cabinet that was remodeled for this work. For this test the cabinet served as the stable holding fixture. The Photodyne power meter was used as the measuring device. The light collector used was the optic fiber with SMA connectors at both ends that was discussed in section II of this chapter. The test setup was very similar to that of Figure 11. A grid with angle markings was made and placed such that with the fiber

connectors installed and the power meter was the same Photodyne Model 11XE. The optical source was the optical communications system constructed with the Augat LED. Optical power readings were taken at every 90° of rotation and the test repeated five times for each end of the fiber. The results were consistent and are listed in Table XI.

Table XI

Connector Loss Measurements					
Fiber End	Position				
	0°	90°	180°	270°	360°
A	-8.9	-8.8	-8.8	-8.9	-8.9
B	-9.5	-10.1	-9.7	-9.4	-9.5
Relative Loss					
A	0	+0.1	+0.1	0	0
B	0	-0.6	-0.2	+0.1	0

All readings listed in Table XI are in dBm and they definitely show that connector A is the better of the two.

The shortcoming of this test is that the actual cause for the losses cannot be determined experimentally. First,

ing was -7.4 dBm. These results gave an attenuation of 3 dB/Km. The manufacturer stated the fiber had an attenuation of 3.8 dB/Km. The results correlate within the limits of the range of the power meter and the amount of fiber available.

Connector Loss. The purpose of this test is to see how well the optical fiber has been attached to the connector in terms of concentricity, facial flatness, and angular misalignment. The absolute loss associated with a connector cannot be measured, but connector losses can be measured and relative comparisons can be made with respect to other connectors and with respect to the different positions in which a single connector can be placed. For this work, connector loss is that referred to in the last context above. The procedure is as follows:

1. Attach on end of the fiber under test to an Optical Power meter.
2. The other end of the fiber is connected to an optical power source.
3. The end of the fiber connected to the optical source is then rotated axially and readings are taken at predetermined positions during the rotation.
4. The readings are then compared to determine the amount of additional loss encountered relative to the axial position of the fiber.

For this work, both ends of the fiber had the OFTI SMA

was used in the test for attenuation. This meter is very portable and has adapters for use with optical fibers that have not had connectors attached. Its only draw back is that it reads only to a tenth of a dBm. Therefore, to get any accuracy a very long piece of fiber must be used.

The procedure for the attenuation test is as follows:

1. Attach one end of the fiber under test to a light source.
2. Measure the amount of optical power exiting the other end of the fiber.
3. Shorten the fiber by some known amount and record the amount of power exiting the fiber again.
4. The difference in the power readings divided by the amount of fiber removed yields the attenuation in dB/m.

In this work one end of the fiber was terminated with an OFTI SMA styled connector and attached to the LED of the newly constructed system. This end of the fiber was not touched during the test. The other end of the fiber was cleaved to give somewhat of a controlled output power pattern for the power meter. This cleaved end was then inserted into the single fiber adapter of the meter and a reading taken. The fiber was shortened, again the end was cleaved, inserted into the adapter and a reading taken.

The initial length of the fiber was 110 meters, and the initial power reading was -7.1 dBm. The fiber was shortened by 100 meters so only 10 meters remained and the second read-

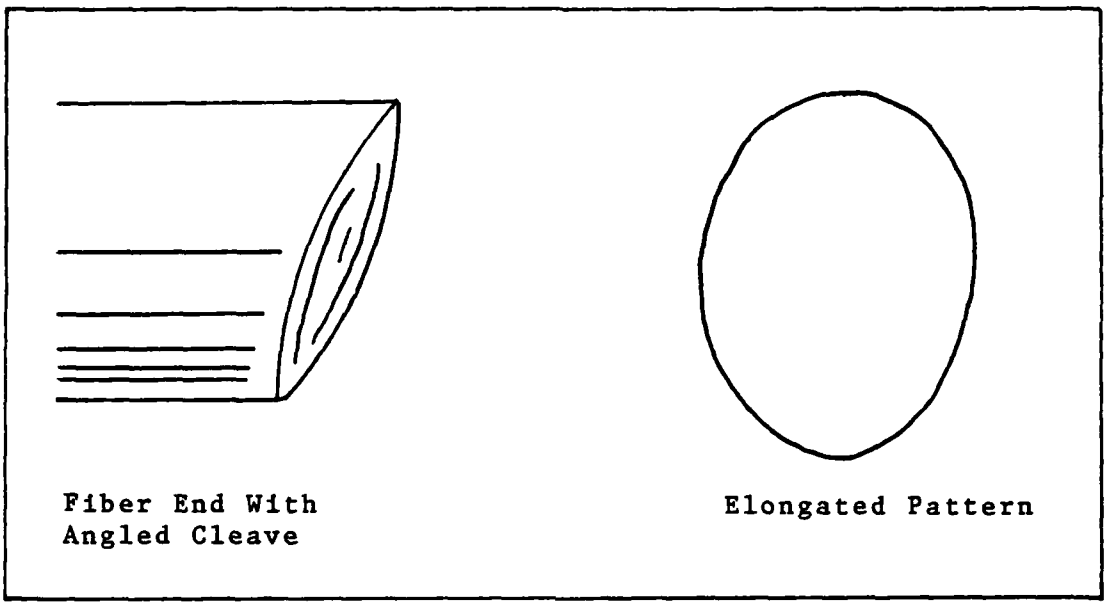

Figure 15c. Light Pattern of Angled Cleave.

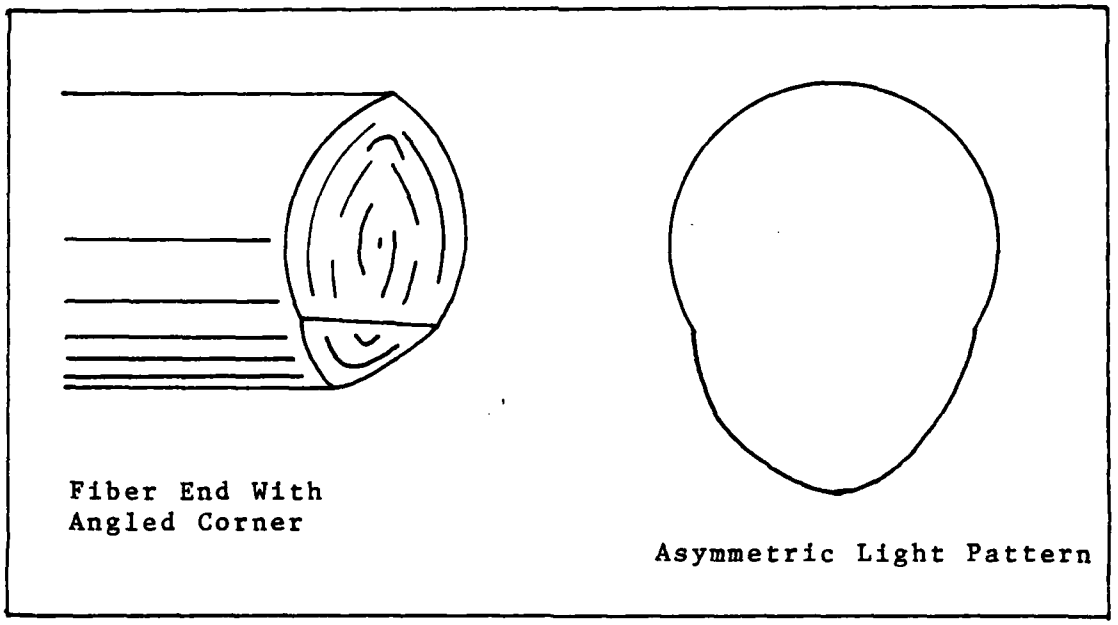

Figure 15d. Light Pattern of Fiber With Angled Corner.

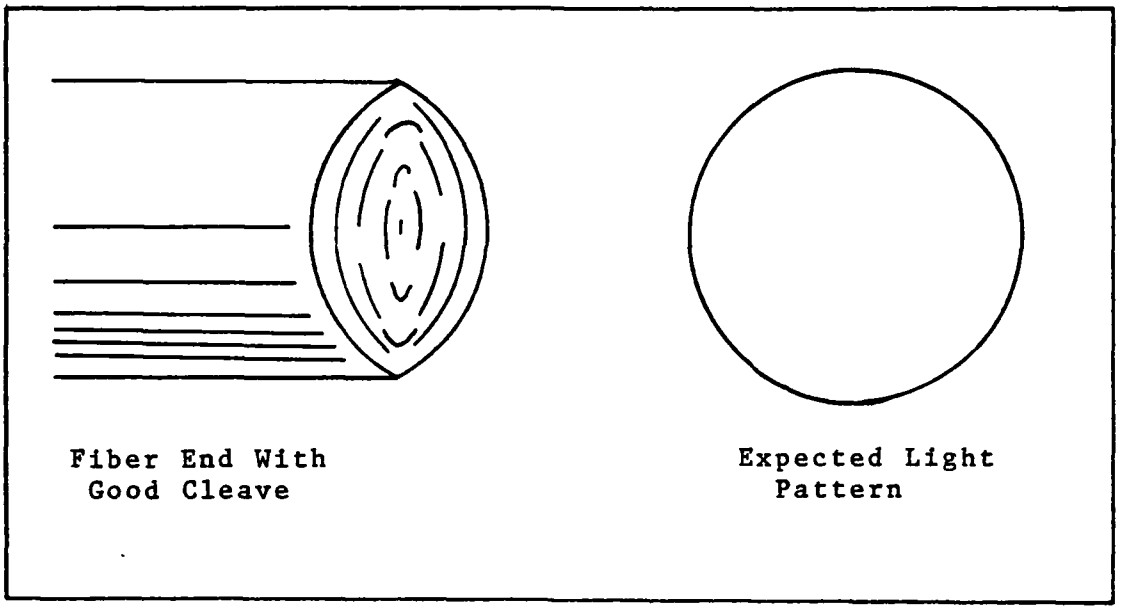

Figure 15a. Light Pattern With Good Cleave.

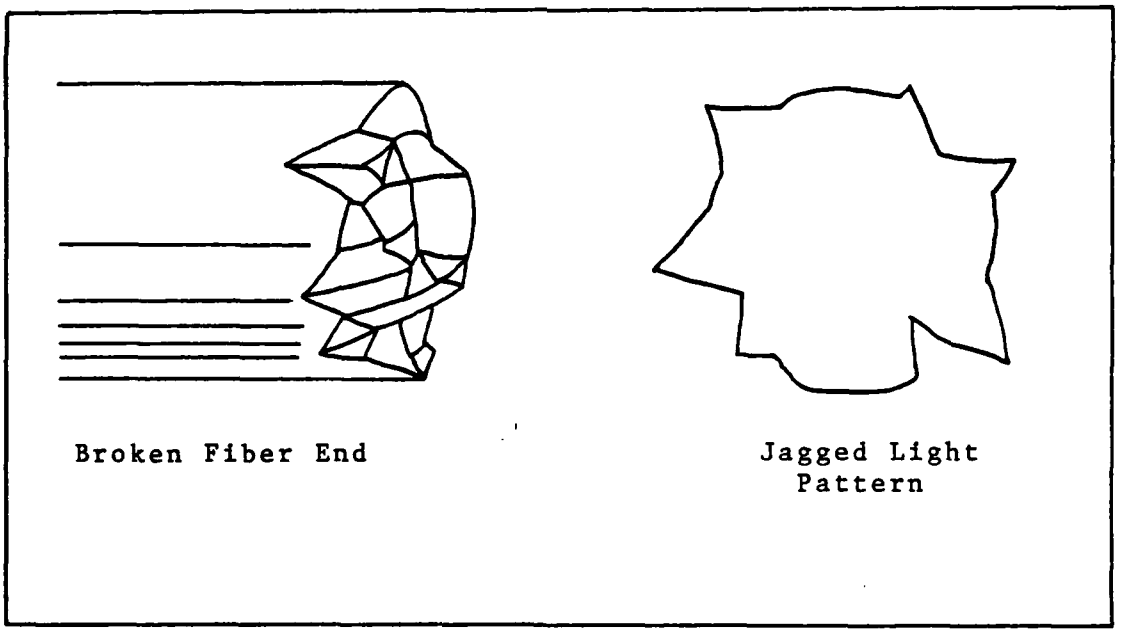

Figure 15b. Light Pattern of Broken Fiber.

putting this end in position for the test, the fiber was apparently broken off close to the cleave. The resulting image on the screen appeared as depicted in Figure 15b. This image was compared to the expected image as shown in figure 15a. The fiber was returned to the microscope and the broken, jagged end was observed.

The next incident was observed on the very next cleave. Again it was thought that a good cleave had been achieved, but when the fiber was positioned at the screen the result was as shown in Figure 15c, and the microscopic inspection revealed the flaw in the cleave. Rather than the face of the fiber being perpendicular to the fiber axis there was an approximate 10° slant on the flat face.

The third case, shown in Figure 15d, was not as easily detected because the flaw in the cleave was so small. The angled corner on the face was eventually discovered and deemed to be the cause of the asymmetric image on the screen.

The results of these three observations show that this test setup can be used to confirm that a good cleave has been achieved. However if the cleave results in a symmetrical concave or convex end this test will not show the results as dramatically, and depending on the urgency of a good cleave, the time, effort, and equipment required for this test may make it impractical.

Fiber Attenuation. A Photodyne, Inc., Model 11XE, portable, digital readout in dBm, Fiber Optic Power Meter

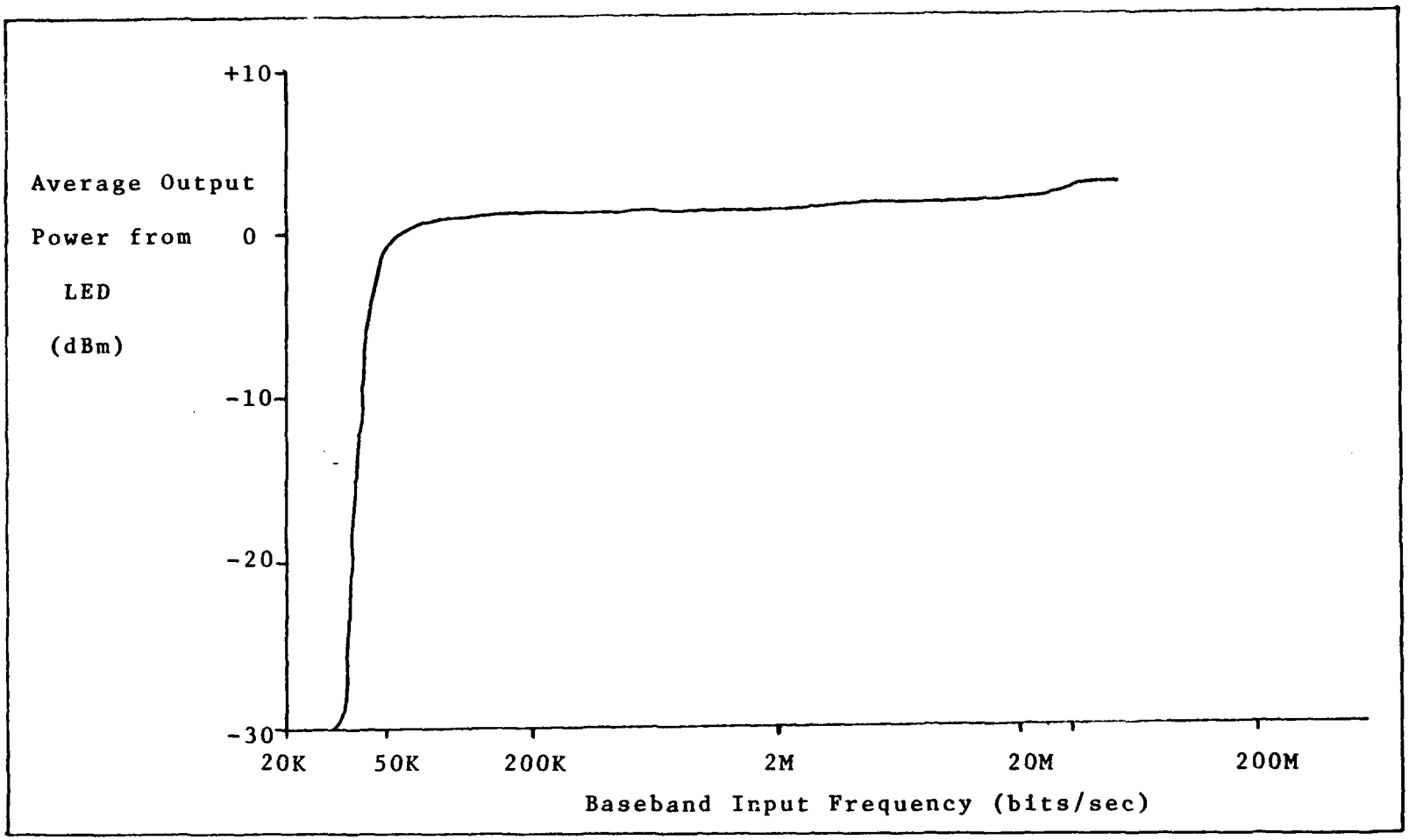

Figure 17. Average Output Power vs Input Frequency.

VI, Conclusion

Information presented in this chapter is broken down into three categories. First, a summary of the work done to upgrade the Spectronics Fiber Bundle System to a single strand optical fiber communications system. Second, problems encountered during this project. Third, recommendations for future work on this system and susggestions for its use as designed in this work.

Summary of Work

Before the feasibility study was conducted towards upgrading the Spectronics system research was conducted into the properties of optical fibers and their use as a communications media. Foremost of the fiber's characteristics in this use is its power losses. Significant losses occur at the power launching point and any connecting points from fiber to fiber. Losses at either the launching or connecting points arise primarily from geometric dimensions and alignment. The three major causes are axial displacement, angular misalignment and longitudinal separation. The inherent, or intrinsic, losses associated with an optical fiber are absorbtion, scattering and radiation.

The feasibility study of upgrading the original system was conducted with the ideas of converting the system to single strand system with maximum utilization of existing equipment and minimum additional cost. It was determined that the

cabinets, power supplies and five of the original circuit cards could be retained and used in the new system. The components that were to be replaced were the fiber optic bundles, the LED, PD and the alignment mounting, the front panel of the cabinet and the four circuit cards that controlled the system's protocol and coding scheme.

Since there was some optical fiber on hand, the only parts that had to be ordered were the LED's, PD's and fiber connectors. Front panels were also ordered to be fabricated in the AFIT Machine Shop. All other parts were either reused from the old system or were locally available including required test equipment.

A modulation/demodulation circuit board was designed and constructed that enabled the system to transmit either baseband or carrier modulated signals. The circuit was also designed to use either an externally provided carrier or an internal 20 MHz carrier. When completed this circuit was tested and functioned exactly as was intended.

When the LED's and PD's arrived they were mounted on the new front panel along with three BNC connectors and three switches which provide all interface and control of the system. The mod/demod circuit board was installed and the connectors were attached to the test fiber. Once the system was intact continuity and functional tests were performed before system characterization commenced.

Component and system level testing was conducted on this fiber optic link. The optical fiber was tested for numeric

aperture, attenuation and connector loss. The LED was profiled by its emission radiation pattern. And finally, the system was put in operation and tested for output power versus frequency, functional operation and frequency response.

The results of these tests showed the fiber to have a loss of 3 dBm/Km, adequate connector efficiencies and a numeric aperture of 0.184. The full width half max angle of the LED was measured to be 6°, and its output power levels were relatively flat from 50 Kbit/sec to 20 Mbit/sec. The system faithfully duplicated the input signal in the baseband mode from 80 Kbit/sec to 20 Mbit/sec, and also operated well in the external carrier mode within the same bandwidth. The internal 20 MHz (40 Mbit/sec) carrier modulation mode did not work because of the upper frequency cutoff of the post detection amplifier and signal conditioning circuits.

The results of this effort are two single strand fiber optic transceivers that can be looped back to themselves or connected to each other to form a full duplex digital communications link capable of transmitting baseband or externally provided carrier modulated signals from 80 Kbit/sec to 20 Mbit/sec. They have TTL compatible inputs and outputs via BNC connectors and the fiber interface is through a standard SMA styled fiber optic connector. The only external power required is a standard 110 V ac source. An Operations Manual has been prepared for future use of this equipment and is contained in Appendix A.

Problems Encountered

Only two problems were encountered in this effort. First, the LED's, PD's and fiber connectors were seven weeks late in being delivered. As much of this time as possible was allotted to investigating the frequency limitations of the LED driver and post detection amplifier and circuit conditioning circuitry. The second problem arose when trying to simulate the completed system and some locally available LED's and PD's were temporarily connected to the system. One of the PD's came in a panel mounting fixture with the case of the PD connected to the anode of the diode. When the case was grounded it also grounded the negatively biased input to the post detection amplifier blowing the input to the transistor. A replacement IC was removed from a surplus amplifier card and installed in the system. The problem was not just detecting the faulty IC, but that the manufacturer had soldered the IC to the circuit board and had other components soldered across raised leads of the IC. When the new one was installed, an IC socket was used and the other components were installed on the opposite side of the circuit board.

Recommendations

The recommended uses for this system are that of a very portable wideband digital communications link for the sole purpose of data transmission or as a media on which different

modulation or coding schemes can be sent for performance, signal to noise or bit error rate analysis.

It is acknowledged that the 20 Mbit/sec bandwidth limitation does not even approach the limitations of current technology in fiber optics, LED's and laser diodes. However, because of the high frequency cutoff of the existing LED driver and post detection amplifier circuits it is not recommended to try to replace the LED with a faster light source. These circuits could not support speeds of hundreds of megahertz much less the gigahertz rates that the optical fibers can transmit.

Appendix

The following 13 pages constitute the user's Operation Manual that was prepared for future use of the fiber optic system described in this project. A copy on this manual has been left with each of the two units constructed.

Operation Manual

20 Mbps Fiber-Optic Communications Link

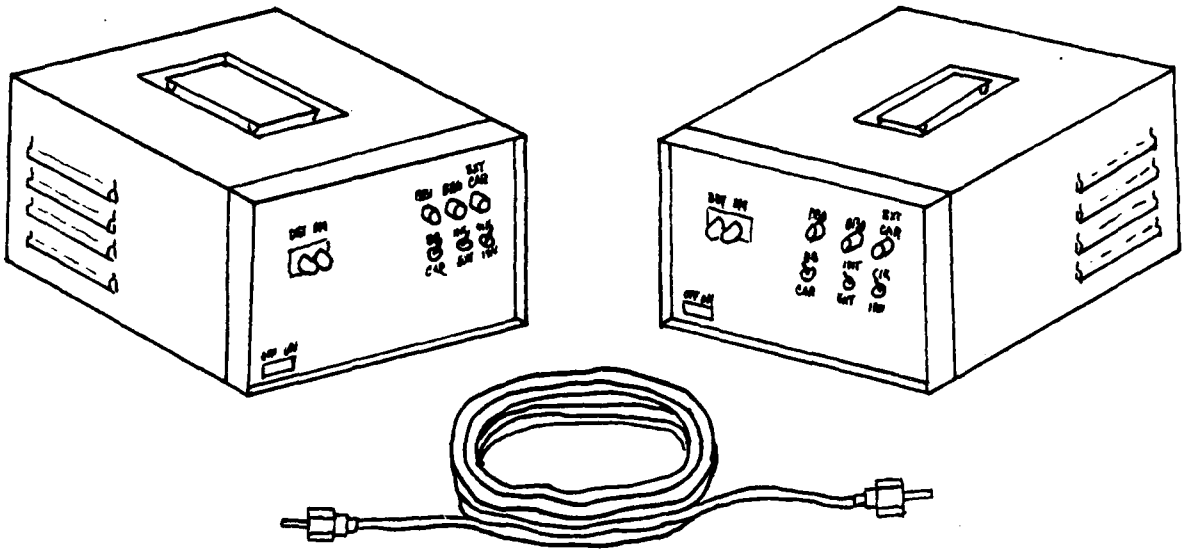

- 80 Kbps - 20 Mbps Bandwidth
- Half/Full Duplex Operation
- TTL Compatible
- Standard SMA Fiber Interface
- Baseband or Carrier Modulation
  - Internal or External Carrier

This manual contains a technical description and operational information for this 20 Mbps Fiber-Optic Communications Link. This manual is broken down into four parts. Section 1 is the technical description of the system. Section 2 covers the theory of operation. Section 3 is the funtional description and directions for operation. And Section 4 contains the schematics for all internal circuits except for the power supplies, ECL Clock card, ECL/TTL Translator card and the forced air cooling system.

Section 1.

This fiber optic data link is capable of transmitting digital signals within the range of 80 Kbps to 20 Mbps. The system has two basic modes of operation: simple baseband or carrier modulation transmission. In the carrier modulation mode either externally provided or internal carriers may be used. Externally modulated signals can also be transmitted by using the baseband mode of operation.

Electrical interface to the user's terminal equipment is provided through standard BNC connectors on the front panel. All inputs and outputs have TTL signalling levels. Transmission mode selection is accomplished through the three switches located directly below the BNC connectors on the front panel.

The optical interface is provided by a bulkhead mounted Light Emitting Diode (LED) and Photodiode (PD). Both the LED and PD have SMA styled receptors compatible with any

standard SMA styled fiber-optic connectors.

SPECIFICATIONS:

Power Requirements - 110 V ac., 60 Hz, 1ø.

Electrical Signallying Interface - Standard TTL, through BNC connectors.

Optical Interface - Single strand optical fiber terminated with SMA styled fiber optic Connectors.

OPTICAL CHARACTERISTICS:

LED - Augat 698-013EG2
Edge Emitting LED
Specifications at 25° C., V_{cc} = 5.0V

Min Reverse Breakdown Voltage	3.0 V
Foward Voltage, I_f = 100 mA	1.9 V
Wavelength	880 nm
FWHM	40 nm
Response Time	20 ns

LED Output Emission Radiation Pattern

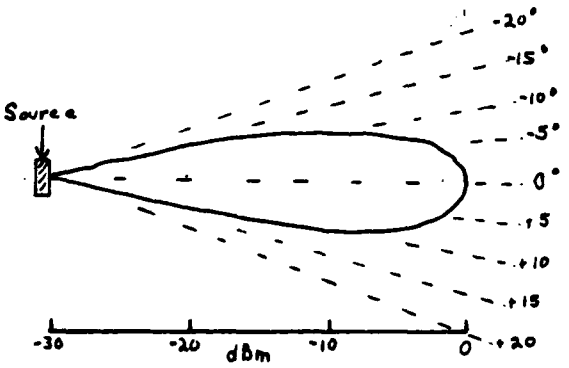

FWHM = 6°

LED Output Optical Power vs Input Baseband Bit Rate

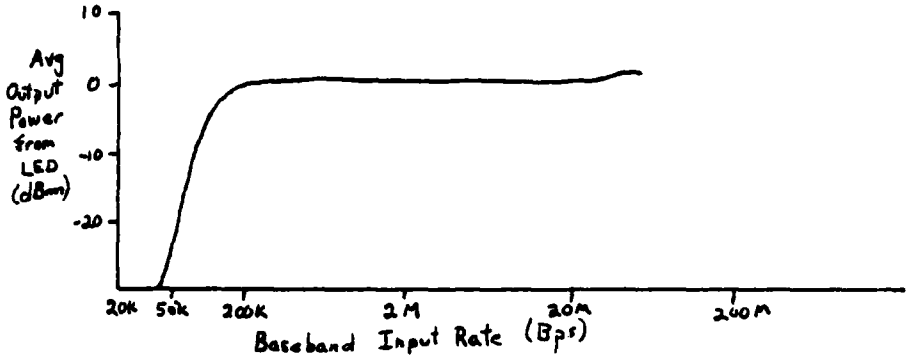

PD - Augat 698-069DG1

p-i-n, coaxial package

Specifiactions at 25° C., V_{cc} = 5.0V, V_{bias} = 50V

Active Area	0.105 X 0.043 in
Reverse Bias	100 V
Dark Current	20 mA
Capacitance	18 pf
Response Time	3.8 ns
Responsivity, @ 880 nm	0.53 A/W
NEP, @ 1 KHz	10^{-13} W/Hz$^{1/2}$

Overall System Bandwidth - 80 Kbps - 20 Mbps.

Section 2.

The following block diagram depicts the signal flow through each of the two units in this fiber optic system.

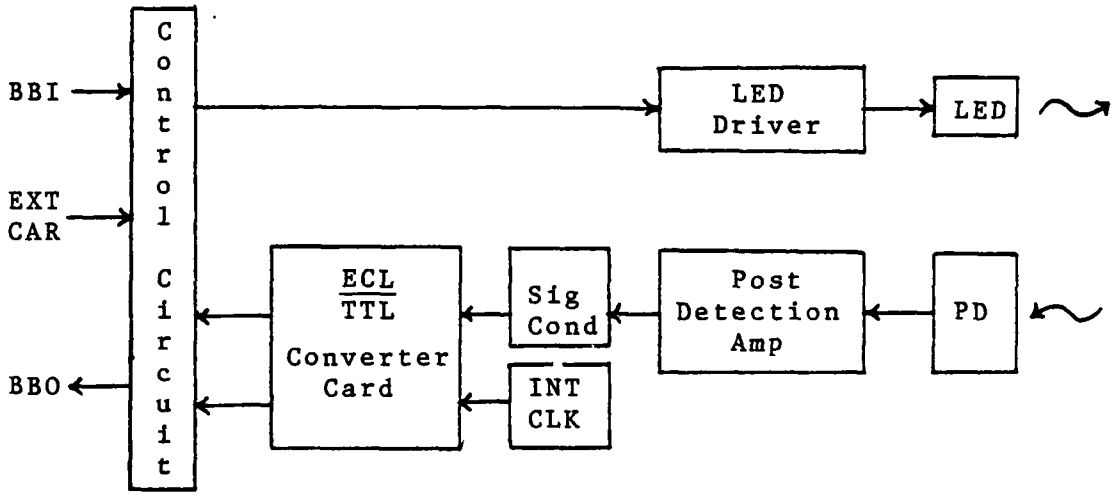

On the transmit side, the baseband signal is connected directly to the LED Driver except when the system is in the carrier mode. In the carrier mode, the baseband signal is AND'd with either the internal clock or external carrier signals by the control circuit and then connected to the LED Driver.

The LED Driver is a two part circuit providing both a current sink for the LED and a capacitive network used as a speed-up circuit that effectively cuts the rise time of the LED in half.

The detected optical signal is first amplified by the post detection amplifier and then goes through the signal conditioning circuit which regenerates a square waveshape proportional to the incoming digital signal. The output of this conditioning circuit is low level and therefore goes through the ECL/TTL Translator card to make the signal TTL Compatible. If the system is in the baseband mode then the

received signal is connected directly to the output. If the system is in the carrier mode, then the received signal goes into a D-flip/flop that is triggered by either the internal clock or external carrier, selected by the INT/EXT selector switch. If the carrier signal is present then the D-flip/flop eliminates the low half of the period by remaining high for the entire carrier period. If the carrier is not present, the output of the D-flip/flop remains low intil the carrier returns. This circuit effectively demodulates the carrier signal and then connects the signal to the output. However, this demodulator circuit depends on very accurate local carrier frequencies.

Bandwidth limitations for this system stem from the frequency response of both the LED Driver and the Post Detection Amplifier and Circuit Conditioning circuits.

Section 3.

This fiber-optic system has three major useful configurations. First, a single unit can be looped back to itself for local testing of a single fiber. Or the two units can be connected with a single optical fiber to establish a simplex mode of operation. Lastly, the two units can be connected with two fibers to comprise a full duplex communications link, with each side (transmit or receive) capable of sending up to 20 Mbps independently.

Each of these three configurations can support both modes of transmission; that is, direct baseband or carrier modulation. To transmit either straight baseband or an externally modulated digital signals such as PDM, PPM or PCM connect the input signal to the BBI BNC connector and put the BB/CAR switch in the BB position. To transmit a carrier modulated signal using the internal carrier connect the baseband signal to the BBI BNC connector and put the BB/CAR switch in the CAR position and the INT/EXT switch in the INT position. To transmit a carrier modulated signal with an externally provided carrier frequency again the baseband goes to the BBI connector, the BB/CAR switch goes to the CAR position, but the INT/EXT switch goes to the EXT position while the external TTL carrier signal is connected to the EXT CAR BNC connector.

When the BB/CAR switch is in the BB position the other two switches have no impact on the transmission regardless of their positions. The CLK/INV switch is used as a simple receiver synchronizer in either carrier modulation modes. If, because of propagation delays, the demodulation circuit is sampling the incoming signal in the low state of the carrier period then the output of the system will always be low. Changing the sense of the CLK/INV switch causes an effective 180° phase shift in the sampling signal and the carrier is then sampled in the high part of its period and can then recreate the baseband signal. Therefore if the system is in the carrier modulation mode and the output remains low, changing the position of

AD-A151 704 WIDEBAND FIBER OPTIC COMMUNICATIONS LINK(U) AIR FORCE INST OF TECH WRIGHT-PATTERSON AFB OH SCHOOL OF ENGINEERING J R BRAY DEC 84 AFIT/GE/ENG/84D-16 2/2

UNCLASSIFIED F/G 17/2 NL

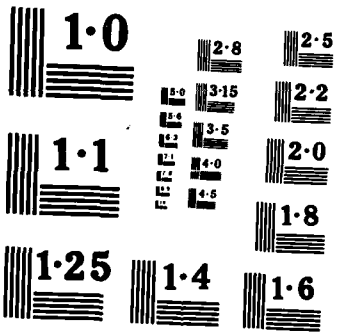
1·0
1·1
1·25
1·4
1·6
1·8
2·0
2·2
2·5
2·8
3·15
3·5
4·0
4·5
5·0

the CLK/INV switch should establish proper demodulation of the signal.

This simple synchronization of carrier demodulation depends on exact external carrier frequencies. The incoming optical signal, after being detected, is sampled at the carrier frequency selected by the INT/EXT switch. When the internal carrier is used, the clock in the receiving unit is exact enough to perform this operation. However, in the external carrier mode there is no carrier tracking or synchronization circuits and the signal is sampled at the rate provided by the external carrier signal. Therefore in a laboratory environment the same external carrier should be provided to each of the units to avoid this shnchronization problem, and a long haul configuration of these two units in the external carrier modulation mode is not feasible.

Section 4.

This section contains schematics for the Control Circuit, the LED Driver, the Post Detection Amplifier and the Circuit Conditioning Cards. Schematics are not included for the two remaining circuits because only the 20 MHz clock signal is used from the bottom card and two ECL/TTL convertors are used from the middle card. All logic gates on the Control Circuit are standard TTL IC's, and on the other schematics all resistance values are in ohms and all capacitance values are in microfarads.

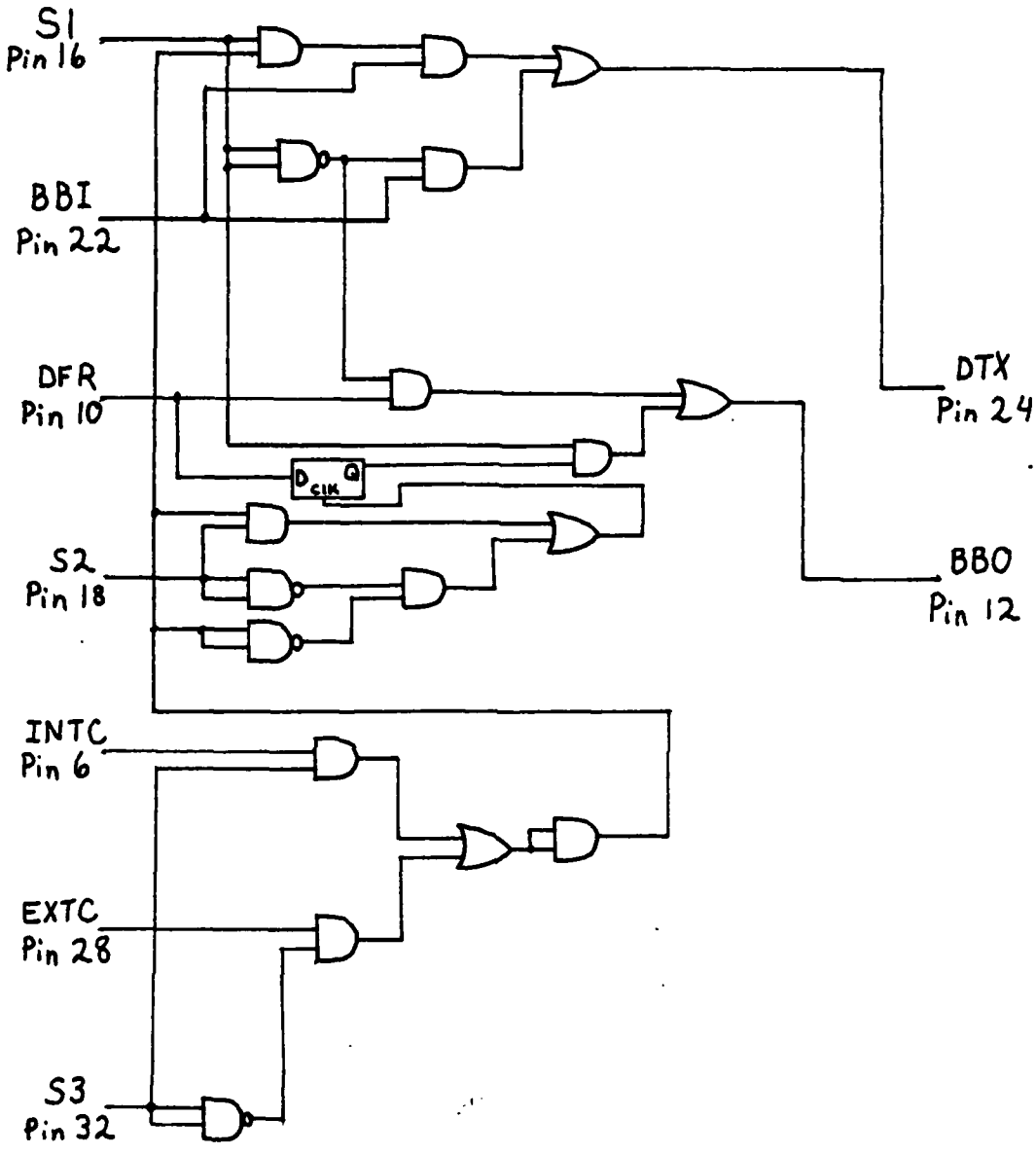

Control Circuit

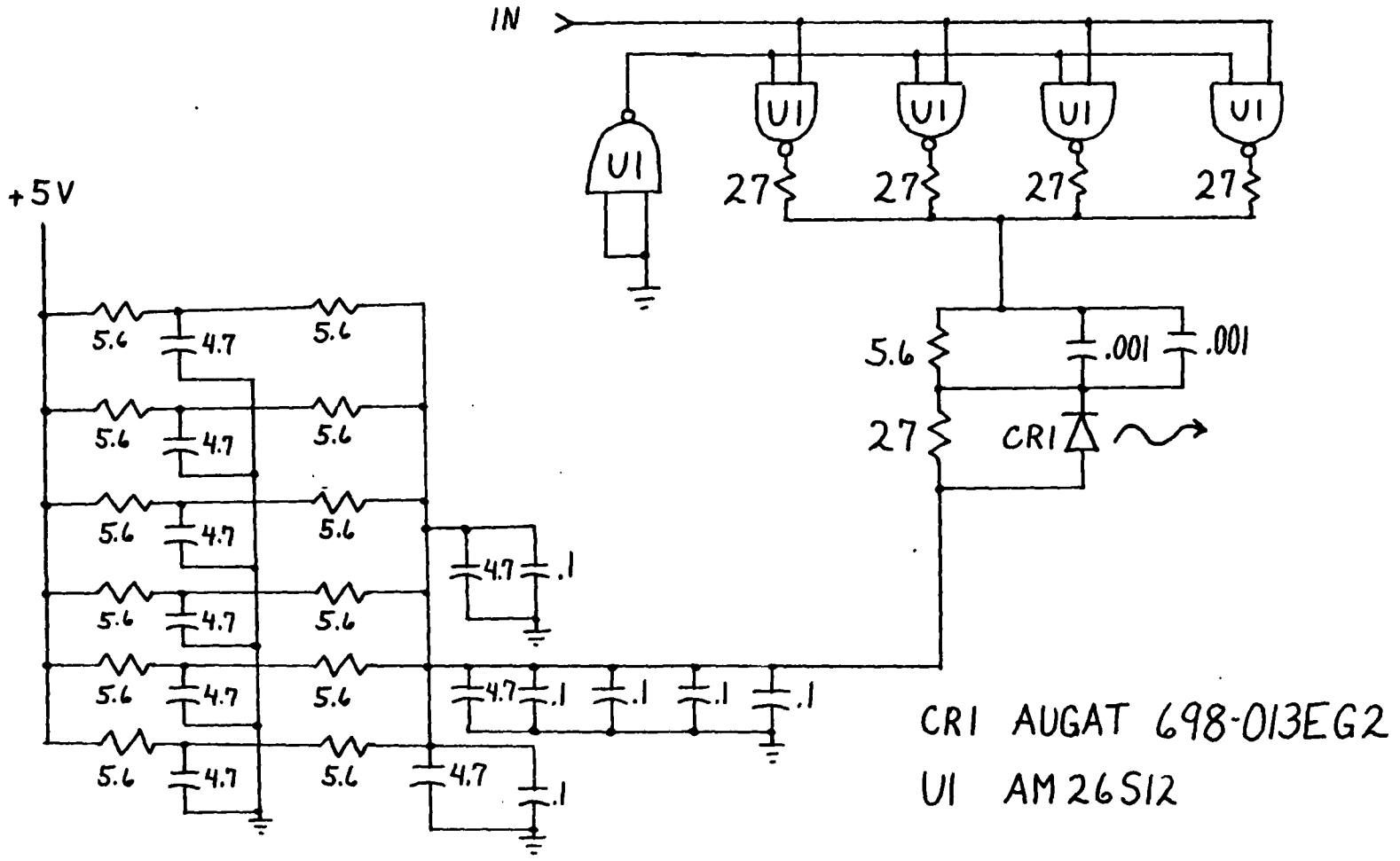
IN
U1
U1
U1
U1
U1
27
27
27
27
+5V
5.6
4.7
.001
.001
CR1
.1
CR1 AUGAT 698-013EG2
U1 AM26S12

LED Driver

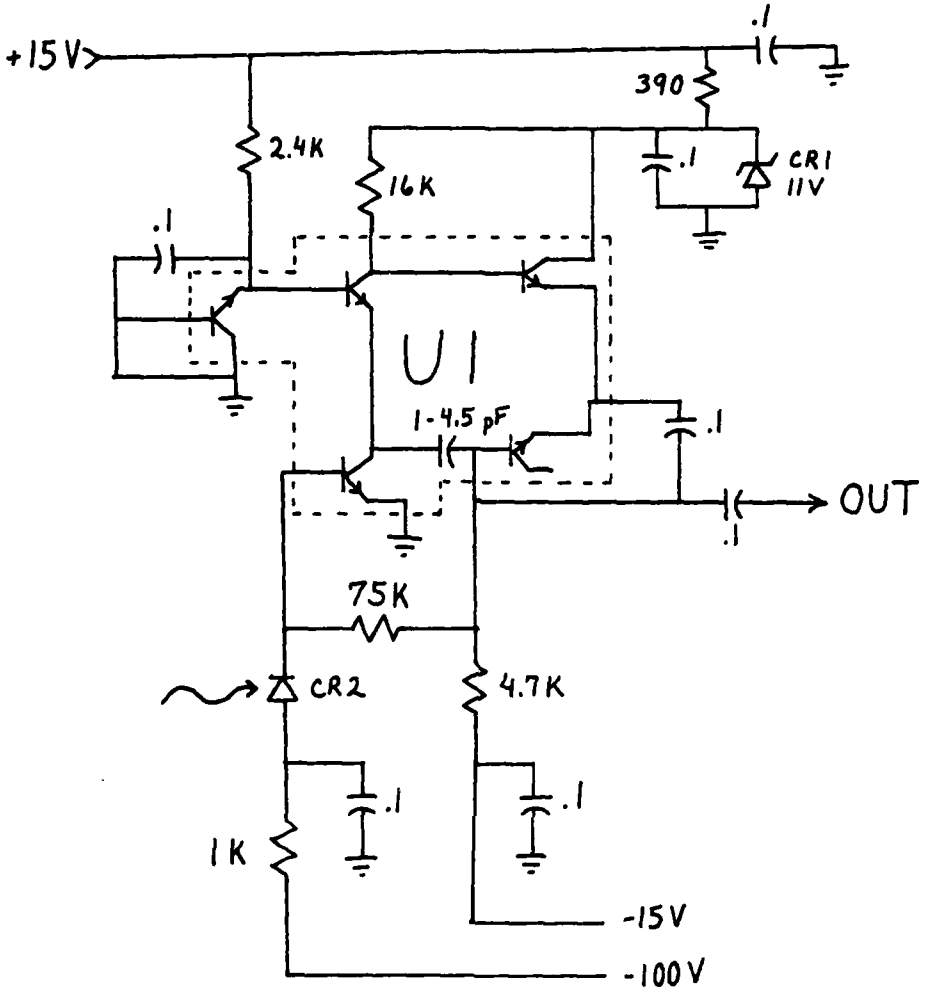

CR1	IN5241
CR2	AUGAT 698-069DG1
U1	RCA-CA3127E

Post Detection Amplifier

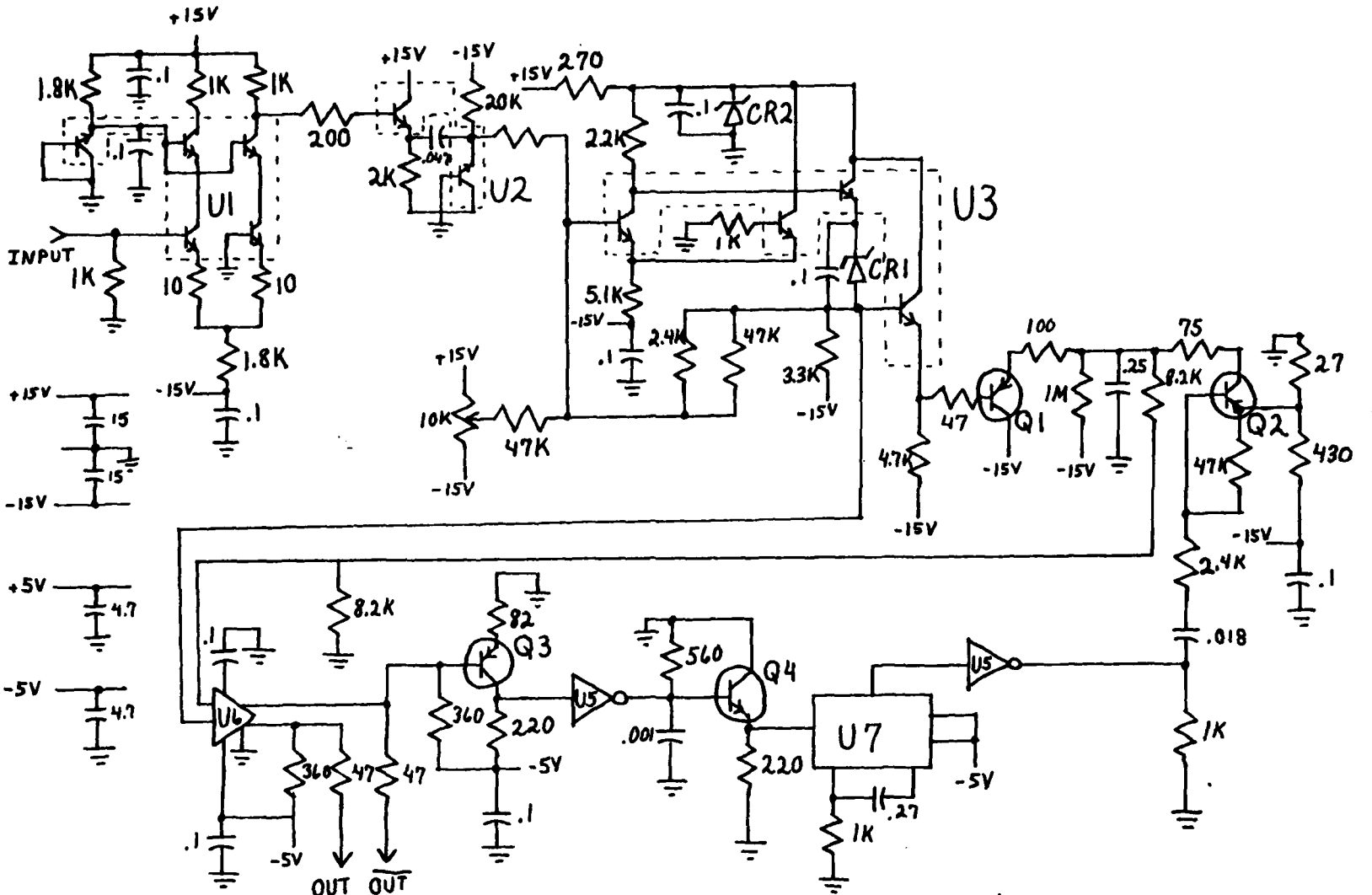

Circuit Conditioning Card

Circuit Conditioning Card

Q1	2N4959
Q2, Q3	2N3906
Q4	2N3904
CR1	TRW PD6205
CR2	IN5241
U1, U2, U3	CA 3127E
U5	7406
U6	AM685DL
U7	74121

Bibliography

1. Air Force Avionics Laboratory, Air Force Systems Command. EMI/EMP Resistant Data Bus. Report from Spectronics, Inc., Richardson, Texas. AFAL-TR-76-99. Contract Number F33615-74-C-1001, September, 1976.

2. Air Force Avionics Laboratory, Air Force Systems Command. Fiber Optic Link Improvement Program. Report from Spectronics, Inc., Richardson, Texas. AFAL-TR-76-128. Contract Number F33615-77-C-1226, August, 1978.

3. Air Force Avionics Laboratory, Air Force Systems Command. Flight Operational Wideband Fiber Optic Data Links. Report from Spectronics, Inc., Richardson, Texas. AFAL-TR-77-54. Contract Number F33615-76-C-1047, November, 1977.

4. Air Force Avionics Laboratory, Air Force Systems Command. Wideband Fiber Optic Data Links. Report from Spectronics, Inc., Richardson, Texas. AFAL-TR-77-55. Contract Number F33615-74-C-1160, October, 1977.

5. Doyle, Hank and Robert A. Wey. Augat Fiberoptics. Design and Operation of a Stable Attenuation Measurement System, May 1982. Augat Fiberoptics Components and Systems, Attleboro MA. 1982.

6. Duke, David A. and others. Optical Waveguide Performance/ Cost Relationship: Special Report, undated. Telecommunications Products Dept., Corning Glass Works, Corning, New York.

7. F122-00077. Amphenol Fibre Optic Designer's Handbook. Product Catalog. Amphenol, Broadview IL, September 1982.

8. Fujii, Y. and others. "Precise Angular Misalignment Measurement in Optical Fiber Connector Plugs," Progress In Optical Communications, Vol I: 158-159 (1980).

9. Horiguchi, M. "Spectral Losses at Low-OH-Content Optical Fibers," Progress In Optical Communications, Vol I: 79-80 (1980).

10. Keck, Donald B. "Single-mode Fibers Outperform Multimode Cables," IEEE Spectrum, Vol 20 : 30-37 (March 1983).

11. Keiser, Gerd. Optical Fiber Communications. New York: McGraw-Hill Book Company, 1983.

12. Kurokawa, T. and others. "Precisely Moulded Plastic Splices for Optical Fibers," Progress In Optical Communications, Vol II: 147-148 (1982).

13. LD-281BR. Light Emitting Diode. Product Description. Laser Diode Laboratories, New Brunswick NJ, undated.

14. LD-281CR. Laser Diode. Product Description. Laser Diode Laboratories, New Brunswick NJ, undated.

15. Noane, G. Le. "Low-Loss Optical-Fiber Sonnection Systems," Progress In Optical Communications, Vol I:114-115 (1980).

16. Osanai, H. and others. "Effects of Dopants on Transmission Loss of Low-OH-Content Optical Fibers," Progress In Optical Communications, Vol I: 80-81 (1980).

17. Rome Air Developement Center, Air Force Systems Command. Optical Cable Communications Study. Report from Harris Corporation, Melbourne, Florida, RADC -TR-75-187. Air Force Contract Number F30602-74-C-0193, July, 1975. (AD-A 016846).

18. Satellite Branch, Communications Engineering Directorate, US Army Communications-Electronics Engineering Installation Agency. Design Handbook for Optical Fiber Systems. Project Order Number CC-006-78. August, 1978. (ADA 061125).

19. Sudo, S. and others. "Low-OH-Content Optical Fiber Fabricated by Vapour-Phase Axial-Deposition," Progress In Optical Communications, Vol I: 103-104 (1980).

20. S104. Shortform Catalog. Product Catalog. Augat Inc., Attleboro MA, August 1982.

21. Tsujimoto, Y. and others. "Fabrication of Low-Loss 3 dB Couplers With Multimode Optical Fibers," Progress In Optical Communications, Vol I: 157 (1980).

22. Wey, Robert A. General Manager, Augat Fiberoptics. Fiberoptic Communications: Technical Review, undated. Augat Fiberoptic Components and Systems, Attleboro Ma, 1982.

VITA

James Bray was born on 16 August 1950 in Louisville, Kentucky. He graduated from Bishop David Memorial High School in Louisville, Kentucky, in 1968, and enlisted in the United States Air Force in November 1969. He attended Texas Tech University under the Airman Education and Commissioning Program, and he received the degree of Bachelor of Science in Electrical Engineering. Upon graduation, he attended Officer Training School and received a commission. He was assigned as a test engineer in the Directorate of Inertial Engineering, Aerospace Guidance and Metrology Center, Newark AFS, Ohio in May 1981. He then served as Chief, Mass and Dimensional Standards Laboratory in the Directorate of Metrology at Newark until entering the School of Engineering, Air Force Institute of Technology, in June 1983.

Permanent Address: 10803 Torrington Rd.
Louisville, Kentucky 40272

REPORT DOCUMENTATION PAGE

1a. REPORT SECURITY CLASSIFICATION UNCLASSIFIED	1b. RESTRICTIVE MARKINGS
2a. SECURITY CLASSIFICATION AUTHORITY	3. DISTRIBUTION/AVAILABILITY OF REPORT Approved for public release; distribution unlimited
2b. DECLASSIFICATION/DOWNGRADING SCHEDULE	
4. PERFORMING ORGANIZATION REPORT NUMBER(S) AFIT/GE/ENG/84D-16	5. MONITORING ORGANIZATION REPORT NUMBER(S)
6a. NAME OF PERFORMING ORGANIZATION School of Engineering 6b. OFFICE SYMBOL (If applicable) AFIT/ENG	7a. NAME OF MONITORING ORGANIZATION
6c. ADDRESS (City, State and ZIP Code) Air Force Institute of Technology Wright-Patterson AFB, Ohio 45433	7b. ADDRESS (City, State and ZIP Code)
8a. NAME OF FUNDING/SPONSORING ORGANIZATION 8b. OFFICE SYMBOL (If applicable)	9. PROCUREMENT INSTRUMENT IDENTIFICATION NUMBER
8c. ADDRESS (City, State and ZIP Code)	10. SOURCE OF FUNDING NOS. PROGRAM ELEMENT NO. / PROJECT NO. / TASK NO. / WORK UNIT NO.
11. TITLE (Include Security Classification) See Box 19	
12. PERSONAL AUTHOR(S) James R. Bray, B.S., 1st Lt, USAF	
13a. TYPE OF REPORT MS Thesis 13b. TIME COVERED FROM _____ TO _____	14. DATE OF REPORT (Yr., Mo., Day) 1984 December 15. PAGE COUNT 105
16. SUPPLEMENTARY NOTATION	

17. COSATI CODES			18. SUBJECT TERMS (Continue on reverse if necessary and identify by block number)
FIELD	GROUP	SUB. GR.	Optical Communications Fiber Optics Fiber Optics Transmission Lines
17	8		

19. ABSTRACT (Continue on reverse if necessary and identify by block number)

Title: WIDEBAND FIBER OPTIC COMMUNICATIONS LINK

Thesis Chairman: Vaqar Syed, PhD.

Approved for public release: IAW AFR 190-17.

LYNN E. [illegible]
Dean for [illegible] Development
Air Force Institute of Technology (AIC)
Wright-Patterson AFB OH 45433

20. DISTRIBUTION/AVAILABILITY OF ABSTRACT UNCLASSIFIED/UNLIMITED ☒ SAME AS RPT. ☐ DTIC USERS ☐	21. ABSTRACT SECURITY CLASSIFICATION UNCLASSIFIED
22a. NAME OF RESPONSIBLE INDIVIDUAL Kenneth C. Castor, Major, USAF	22b. TELEPHONE NUMBER (Include Area Code) 513-255-5276 22c. OFFICE SYMBOL AFIT/ENG

A feasibility study was conducted on the possibility of upgrading a nine port fiber optic bundle telecommunications system to a single strand fiber optic system. Usable pieces of equipment were identified and new Light Emitting Diodes, Photodetectors and single strand SMA styled fiber optic connectors were ordered. Background research was conducted in the area of fiber optic power launching, fiber losses, connector losses and efficiences. A new modulation/demodulation circuit was designed and constructed using parts from unused equipment. A new front panel was constructed to house the components, switches and connectors. A two meter piece of optical fiber was terminated with the new connectors and tested for connector loss, numeric aperture and attenuation. The new Light Emitting Diode was characterized by its emission radiation pattern and the entire system was tested for functional operation, frequency response and bandwidth of operation. An Operations Manual was prepared to ensure proper use in the future. The result was a two piece, single strand, fiber optic communications system fully TTL compatible, capable of transmitting digital signals from 80 Kbit/sec to 20 Mbit/sec. The system was tested in a half duplex mode using both baseband and carrier modulated signals. Utilizing both pieces of the system full duplex operation was also demonstrated.

END

FILMED

5-85

DTIC